Available online at www.sciencedirect.com
ScienceDirect
Global and Planetary Change 55 (2007) 155–176
GLOBAL AND PLANETARY CHANGE
www.elsevier.com/locate/gloplacha

Biostratigraphy and event stratigraphy in Iran around the Permian–Triassic Boundary (PTB): Implications for the causes of the PTB biotic crisis

H.W. Kozur

Rézsü u. 83, H-1029 Budapest, Hungary

Received 27 June 2006; accepted 30 June 2006
Available online 20 September 2006

Abstract

The conodont succession and stratigraphic events around the Permian–Triassic boundary (PTB) have been investigated in detail in the open sea deposits of Iran (Abadeh and Shahreza in central Iran, and Jolfa and Zal in northwestern Iran). This investigation produced a very detailed conodont zonation from the *Clarkina nodosa* Zone up to the *Isarcicella isarcica* Zone. All significant events have been accurately located and dated within this zonation, and the duration of most of these conodont zones has been calculated by cross-correlation with continental lake deposits that display obvious Milankovitch cyclicity. The unusually short duration of all conodont zones in the interval from the *C. nodosa* up to the *Hindeodus parvus* Zone indicates that there was persistent high ecological stress during this time interval. Most of the conodont zones can be accurately correlated with South China. In the interval from the *C. hauschkei* Zone to the *H. parvus* Zone, even correlation with the Arctic is possible.

Within three thin stratigraphic intervals, the Changhsingian (Dorashamian) warm water conodont fauna of the *C. subcarinata* lineage is replaced by a cool water fauna with small *H. typicalis*, rare *Merrillina* sp., and cool water *Clarkina* that have very widely spaced denticles. The uppermost cool water fauna horizon comprises the lower *C. zhangi* Zone and can be accurately correlated with continental beds by recognition of a short reversed magnetozone below the long uppermost Permian–lowermost Triassic normal magnetozone. In Iran and Transcaucasia, this short reversed zone comprises the upper *C. changxingensis–C. deflecta* Zone and most of the *C. zhangi* Zone. Its top lies 50 cm below the top of the *Paratirolites* Limestone (s.s.) in the Dorasham 2 section, which is at the beginning of the upper quarter of the *C. zhangi* Zone. In the Germanic Basin, this short palaeomagnetic interval comprises the lower and the basal part of the upper Fulda Formation. On the Russian Platform, the Nedubrovo Formation belongs to this short reversed magnetic interval. In its upper part (corresponding to the top of the lower *C. zhangi* Zone, see above) there is a fallout of mafic tuffs from the Siberian Trap event that originated about 3000 km away in eruption centres in the Siberian Tungusska Basin. In the Germanic Basin and in Iran, this horizon contains volcanic microsphaerules. Thus, a direct correlation can be made between the immigration of a cool water fauna into the tropical realm and an exceptionally strong interval of explosive activity during the Siberian Trap volcanic episode. These faunal changes are the same as those found at the base of the Boundary Clay, suggesting that a short cooling event at this horizon also was due to intense volcanism. Additional influence by a bolide impact cannot be excluded.

Most of the events in the interval from the *C. nodosa* up to the *I. isarcica* Zone (upper Changhsingian to middle Gangetian) in the Iranian sections can be also observed in other marine sections (e.g., in Meishan) and even in continental sections of the Germanic Basin.

Of particular significance is the fact that, in the investigated Iranian sections, the PTB lies either in red sediments or in light grey sediments (as in Abadeh) that contain an ostracod fauna indicative of highly oxygenated bottom waters. Therefore, anoxia cannot

E-mail address: kozurh@helka.iif.hu.

0921-8181/$ - see front matter
doi:10.1016/j.gloplacha.2006.06.011

be the reason for the PTB extinction event in this region, even though anoxia does cause locally or regionally elsewhere an overprint on the extinction event.

Keywords: Biostratigraphy; event stratigraphy; Permian–Triassic boundary; Permian-Triassic boundary (PTB); climatic changes; cool water conodont immigration

1. Introduction

Rather deep water sequences around the Permian–Triassic boundary (PTB) have been investigated in several sections in northwestern Iran (Jolfa and Zal areas) and central Iran (Abadeh and Shahreza areas) (Fig. 1A). These sections are all situated on the Sanandaj–Sirjan block of the Cimmerian microcontinent, which was bounded by the Neotethys on its SSW and by the Palaeotethys on its NNE margins (Stampfli and Borel, 2004). The Abadeh and Shahreza areas are on the Neotethyan shelf of the Cimmerian terranes. The Jolfa and Zal areas are on the Cimmerian terranes closer to the Palaeotethys (Fig. 1B).

All sections have an open sea, mostly deeper water fauna that primarily consists of ammonoids, conodonts, brachiopods, echinoderms, ostracods, deep water corals and some bivalves in the Permian part, and ammonoids, conodonts, echinoderms, ostracods and bivalves in the Triassic part. These faunas can be correlated throughout the Tethys region, and elements of them also occur as far away as Madagascar (the *Paratirolites* ammonoid fauna) and Greenland (conodont faunas of the uppermost Permian *Clarkina hauschkei* Zone to the lowermost Triassic *Hindeodus parvus* Zone, and also the *Hypophiceras* ammonoid fauna of the *Clarkina meishanensis–Hindeodus praeparvus* and *Merrillina ultima–Stepanovites* ? *mostleri* Zones).

Upper Permian rocks crop out north and south of the Araxes River west of Jolfa (Julfa, Djulfa, or Dzhulfa) in Azerbaijan and in northwestern Iran. These are classic areas for Late Permian stratigraphy. Historical reviews of the Upper Permian studies in this area have been given by Ruzhentsev and Sarycheva (1965), Stepanov et al. (1969) and Kozur (2005); for references see these papers.

This region includes the type area for the Dzhulfian Stage (Schenck et al., 1941), which has its type area west of Jolfa, and the Dorashamian Stage (Rostovtsev and Azaryan, 1971, 1973) which has its stratotype (Dorasham 2) west of Jolfa and north of the Araxes River.

The Upper Permian sections of central Iranian Abadeh were discovered and studied much later than those around Jolfa. The Abadeh sections were described by Taraz (1969, 1971, 1973, 1974) and by the Iranian–Japanese Research Group (I–JRG, 1981). The sections at Shahreza (central Iran) and Zal (northwestern Iran) were discovered even later and have been described and conodont-dated in detail only recently by Kozur (2005).

The first conodonts from this region were described by Sweet (in Teichert et al., 1973) from Jolfa (uppermost Dzhulfian to lowermost Triassic), and by Kozur (1975) and Kozur et al. (1975) from Jolfa and Abadeh (Capitanian to basal Triassic). The upper Dorashamian and basal Triassic conodonts later were revised and new taxa described by Kozur (2004a). From this database, Kozur (2005) compiled and published a detailed conodont zonation. Additional Capitanian to basal Triassic conodonts from Abadeh and Jolfa have been illustrated by Kozur (1978, 1995) and from Abadeh and Shahreza (Dzhulfian and lower Dorashamian) by Yazdi and Shirani (2002).

The I–JRG (1981) published data on the conodont ranges from Abadeh. Similarly, Sweet and Mei (1999a,b) discussed the ranges of conodonts from the Jolfa sections (in sections 1 and 4 of Teichert et al., 1973) and from Abadeh. Gallet et al. (2000) also have discussed the range of the upper Dzhulfian and Dorashamian conodonts from Abadeh. In these latter papers, no conodonts were illustrated or described.

All events around the PTB can be accurately dated by means of the detailed conodont zonation from the *Clarkina nodosa* Zone up to the *Isarcicella isarcica* Zone. By cross-correlation with continental lake deposits of the Germanic Basin, which contain readily recognisable Milankovitch cyclicity (Kozur, 2003, Bachmann and Kozur, 2004, Kozur and Bachmann, 2005, Korte and Kozur, 2005b), not only can the numerical age of the events be readily established, but the duration of most of the conodont zones also can be calculated. In the *C. meishanensis–H. praeparvus*, *H. parvus* and *I. isarcica* Zones, these data also can be obtained by correlation with shallow water marine deposits, wherein the Milankovitch cyclicity often is well developed.

2. Investigated sections

2.1. Abadeh area

The Abadeh sections (Fig. 3) are situated in Kuh-e-Hambast, 60 km SE of the town of Abadeh. A historical

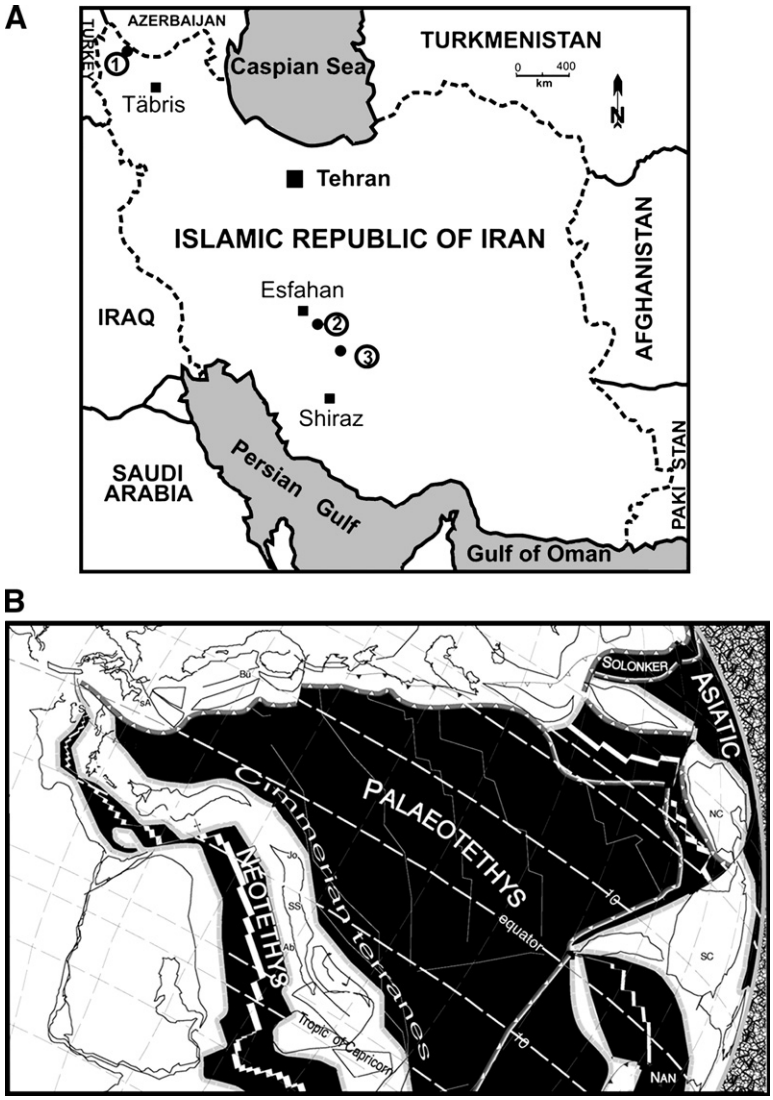

Fig. 1. Studied Iranian regions and their palaeogeographic setting, A: investigated areas in Iran. 1: Kuh-e-Ali Bashi sections, 9 km W of Jolfa, and Zal 22 km SSW of Jolfa, 2.2 km NNW of Zal village. 2: Shahreza section, 14.5 km NNE of Shahreza village, 3.8 km ESE of Shazadeh Ali Akbar village. 3: Abadeh sections, Kuh-e-Hambast, 60 km SE the town of Abadeh. B: Upper Permian (260 Myrs) palaeogeographic reconstruction of the central and western Tethyan Cimmerian terranes with the assumed position of the Julfa/Zal area (Jo) and the Abadeh/Shahreza area (Ab) at the shelves of the Sanandaj–Sirjan block (SS). NC: North China, SC: South China, Bü: Bükk Mts. (Hungary), sA: Southern Alps, Si: Sicanian palaeogeographic domain in western Sicily. Modified after a Tethyan reconstruction for 260 Myrs by Stampfli and Borel (2004). Only the distribution of oceanic and continental crust is shown. Large parts of the Sanandaj–Sirjan block and South China were covered by a shallow to moderately deep sea around the PTB. Bükk Ms. and eastern Southern Alps were covered by a shallow shelf sea and in the Sicanian palaeogeographic realm deep water conditions prevailed around the PTB.

review of the investigation and the development of the lithostratigraphic subdivisions and biostratigraphic dating of these sections is given in Kozur (2005). The lithostratigraphic subdivisions of Baghbani (1993) are used, with the one exception that the base of the Hambast Formation is placed at the base of the *Codonofusiella* Beds of uppermost Unit 5.

The locations of the seven investigated PTB sections are shown in I–JRG (1981, Fig. 3). They are arranged from NW to SE along the sections E, C, B, and A of the I–JRG (1981) study. Sections VI (= section C in I–JRG, 1981) and VII (= section A in I–JRG, 1981) were examined in detail. In the other sections, only the uppermost part of Unit 7 and the lowermost part of Unit "a" across the PTB were investigated, mostly by taking single samples from selected horizons. Denser sampling of this interval was carried out on section I (about 500 m NW of section E

in I–JRG, 1981) and section V (where the PTB interval is in lateral continuity with section E).

2.2. Shahreza area

The Shahreza locality (Figs. 2B, 4) lies 14.5 km NNE of the village of Shahreza and 3.8 km ESE of the village of Shahzadeh Ali Akbar (Fig. 2B). The lithologic subdivisions are similar to those at Abadeh, except that the stromatolites in Unit "a" are not so well developed. As a whole, the water depth is slightly greater in the Shahreza section than in the Abadeh sections.

2.3. Jolfa area

Five sections (Figs. 2C, 5 6) were investigated in Kuh-e-Ali Bashi, about 9 km west of the village of Jolfa in northwestern Iran (Fig. 2C). The Kuh-e-Ali Bashi sequence was described in detail by Stepanov et al. (1969) and by Teichert et al. (1973). A historical review

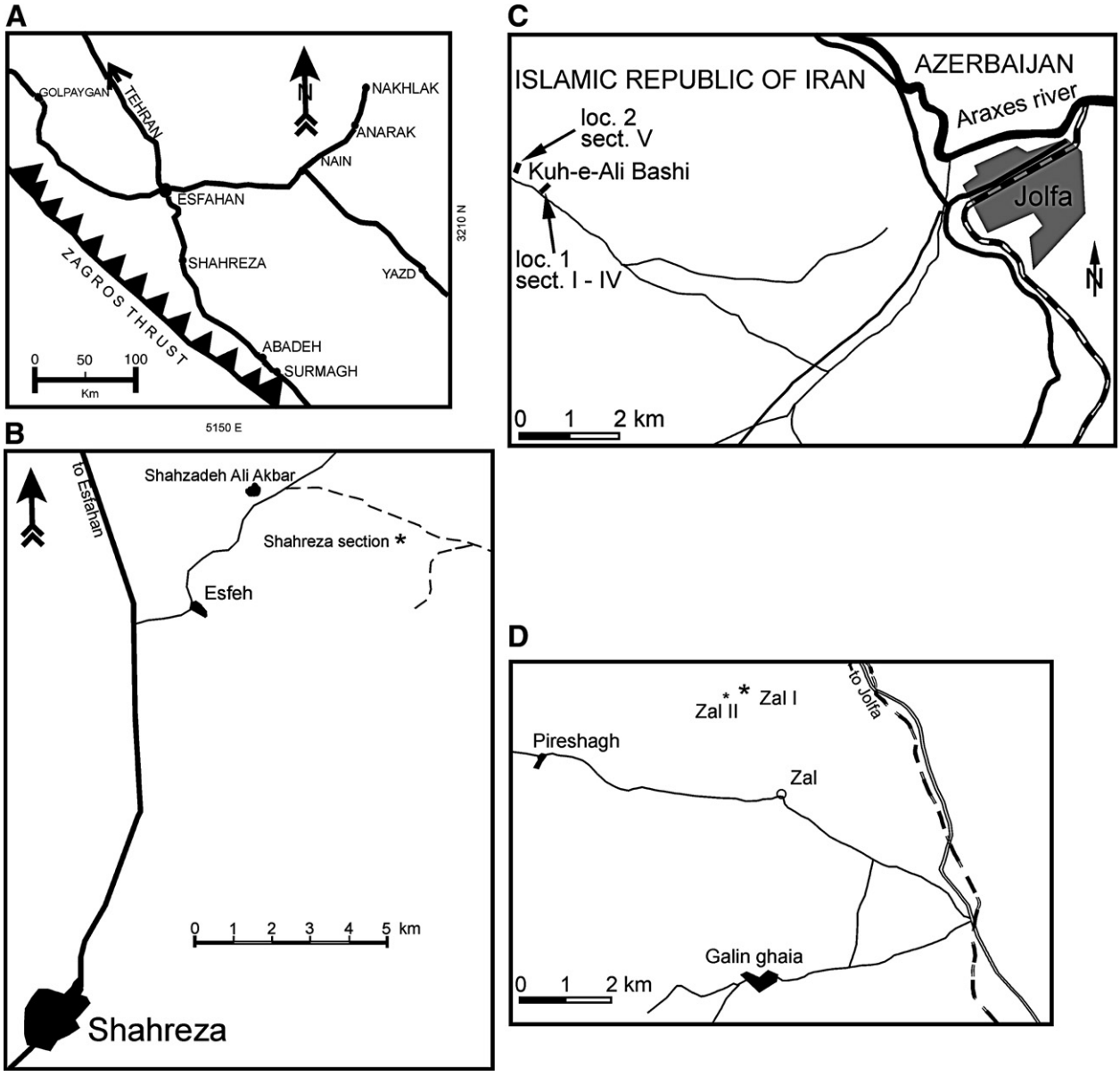

Fig. 2. Locality maps of the investigated sections. A: overview of the Esfahan–Shahreza–Abadeh area in Cental Iran. B: location of the Shahreza section. C: location of the Jolfa sections I–V, Kuh-e-Ali-Bashi, NW Iran. D: location of the Zal sections I and II. All after Kozur (2005).

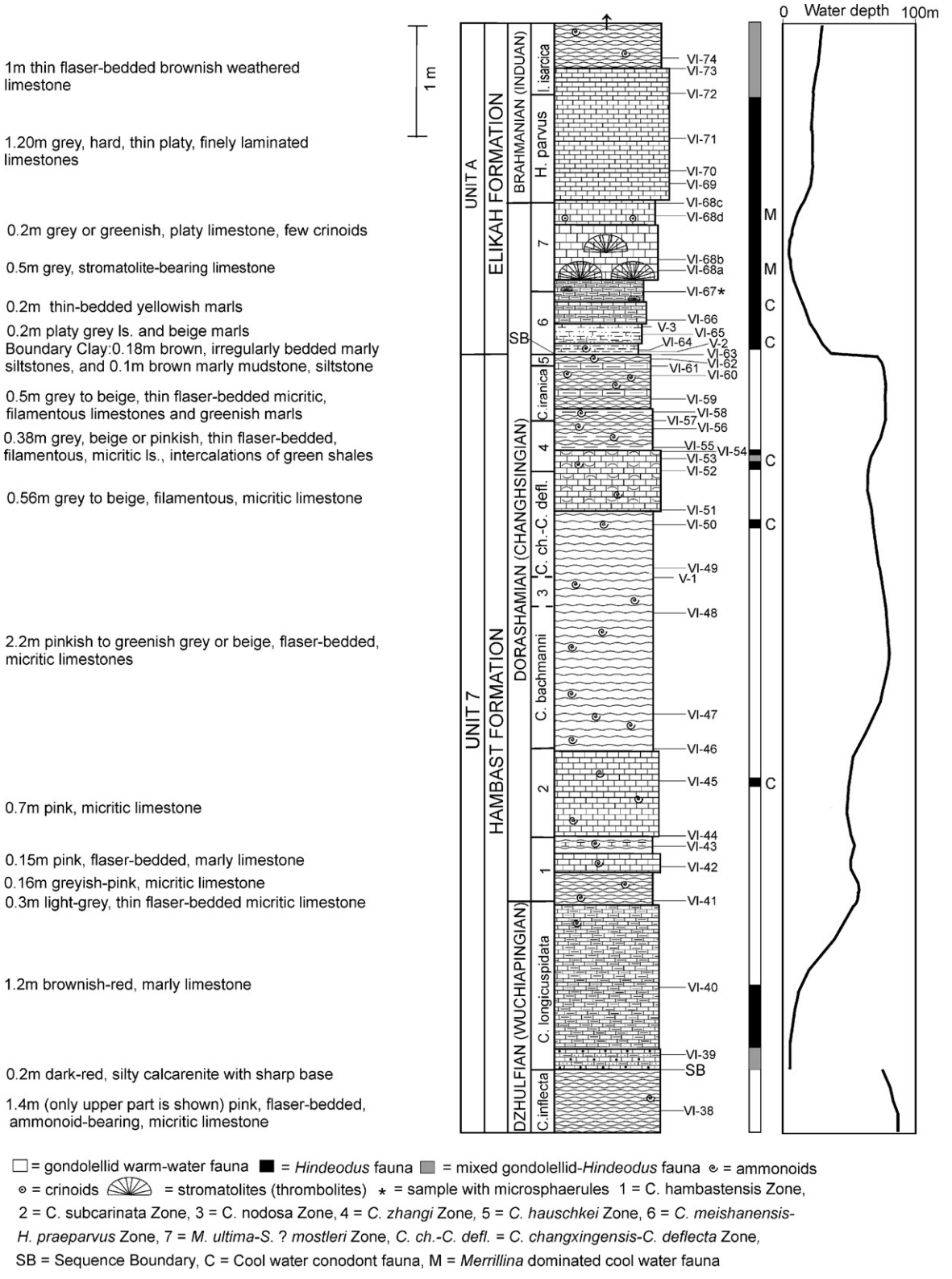

Fig. 3. Lithology, conodont biostratigraphy and water depth of the upper Dzhulfian (Wuchiapingian) to middle Gangetian (lower Brahmanian, Induan) in section VI, Kuh-e-Hambast, Abadeh area, central Iran. The samples V…are not from this section but from section V which has the same thickness and lithology as section VI. Modified after Kozur (2005).

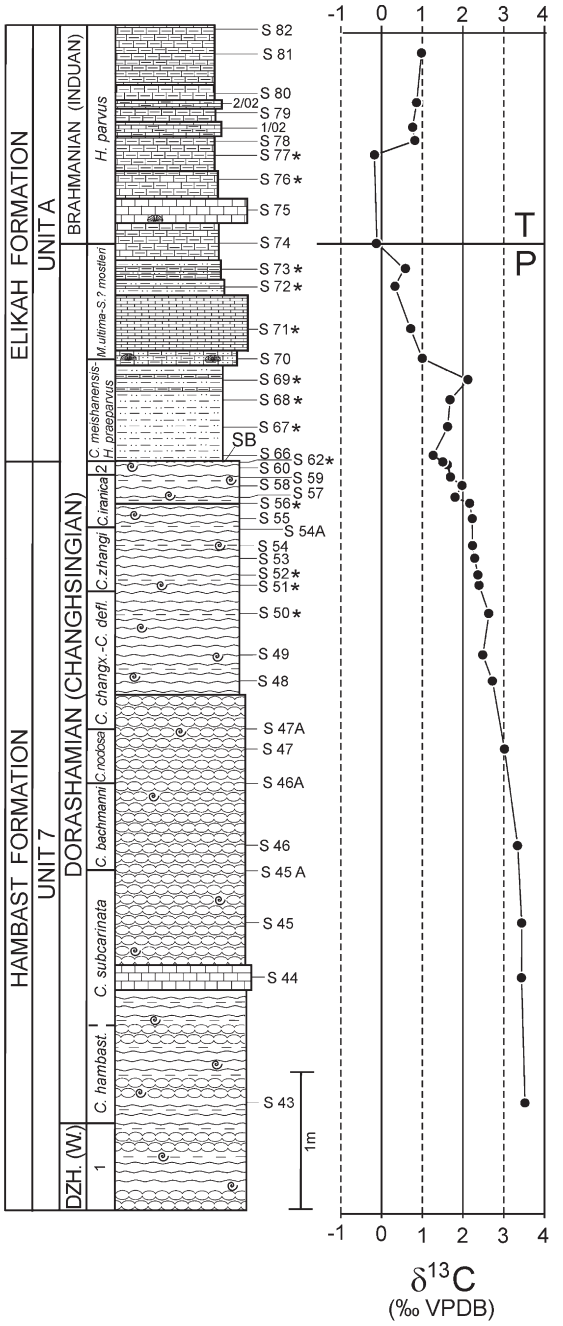

DZH. (W.) = DZHULFIAN (WUCHIAPINGIAN)
= ammonoids = stromatolites
* = samples with microsphaerules
1 = *Clarkina longicuspidata* Zone, 2 = *C. hauschkei* Zone
C. changx.-C. defl. = *Clarkina changxingensis-C. deflecta* Zone
SB = Sequence boundary

Fig. 4. Lithology, conodont biostratigraphy and carbon isotope data in the Dorashamian (Changhsingian) and basal Triassic of the Shahreza section, Central Iran. Modified after Kozur (2005), carbon isotope data after Korte et al. (2004b).

of the investigation and the development of the lithostratigraphic subdivisions and biostratigraphic dating is given in Kozur (2005).

2.4. Zal area

The Zal sections (Figs. 2D, 7) are situated 22 km SSW of Jolfa and 2.2 km NNW of the village of Zal (Fig. 2D). Section Zal I (Fig. 7) is situated at the base of a westward facing slope. It is a continuous section from the uppermost part of the lower Jolfa Formation up into the Lower Triassic. Only the upper Dorashamian to earliest Triassic part was densely sampled.

3. Results and analyses

3.1. Lithostratigraphy

The lithostratigraphy of the Dorashamian is very uniform in central and northwestern Iran and in Transcaucasia. The greater part of the Dorashamian consists of relatively deep water, pink to reddish limestones that contain intercalations (generally thin) of reddish shale. These beds contain ammonoids, small brachiopods, deep water corals, conodonts, ostracods and echinoderms. Together with the lithologically similar underlying late Dzhulfian beds, these Dorashamian beds are assigned to the upper Hambast Formation in the Abadeh and Shahreza sections. In the Jolfa and Zal sections, these beds have more abundant shale and marl intercalations that often are thicker. There they are separated from the lithologically similar upper Jolfa Formation of late Dzhulfian age and assigned to the Alibashi Formation.

In all sections, a strong facies change occurs at the base of the Boundary Clay, which is between 0.27 and 0.28 m thick in the Abadeh sections and 0.90 m thick in the Jolfa sections. At this boundary all brachiopods and corals disappear, as do all warm water ammonoids (*Paratirolites*, *Abichites*, *Pseudogastrioceras*) and conodonts of the *Clarkina subcarinata* lineage. In contrast, the benthos of small foraminifers and ostracods is not significantly affected.

The Boundary Clay and the immediately overlying limestones and marls belong to the uppermost Dorashamian. These beds are assigned to the basal Elikah Formation in all of the investigated central and northwestern Iranian sections. The pink to reddish colour of the underlying beds persists throughout this unit with only one exception; in the Abadeh section the colour changes into grey at the base of the Boundary Clay. Even there, however, a rich and rather diverse ostracod fauna without filter feeders (such as cavellinids and

Hollinella tingi (Patte)) indicates that the bottom waters were well oxygenated. Filter feeders, comprising a very low diversity fauna of 1–3 ostracod species (mostly cavellinids and/or *H. tingi*), dominate around the PTB in all sections that had reduced oxygen content in the bottom waters.

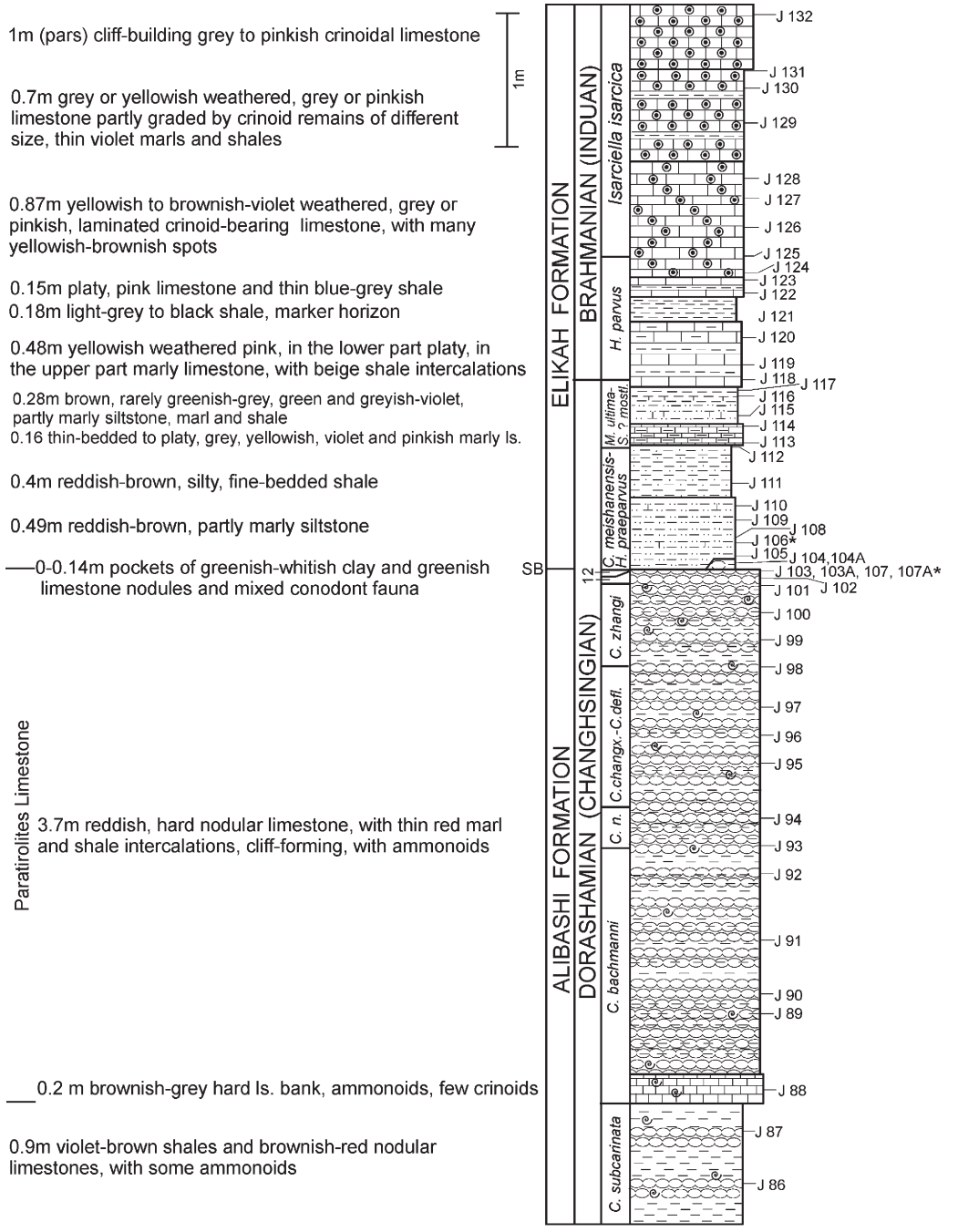

C. n. = *Clarkina nodosa* Zone, *C. changx.-C. defl.* = *C. changxingensis-C. deflecta* Zone,
M. ultima- S. ? mostl. = *M. ultima-S. ? mostleri* Zone, 1: *Clarkina iranica* Zone, 2: *C. hauschkei* Zone
= ammonoids, = crinoids, * = samples with microsphaerules. SB = Sequence boundary
Samples J 103A, 107 and 107A are situated in lateral continuation of sample J 103.

Fig. 5. Lithology and conodont biostratigraphy of the middle-upper Dorashamian and lower Brahmanian (lower and middle Gangetian Substage) of partial section III of locality 1 at Kuh-e-Ali-Bashi, W of Jolfa. Modified after Kozur (2005).

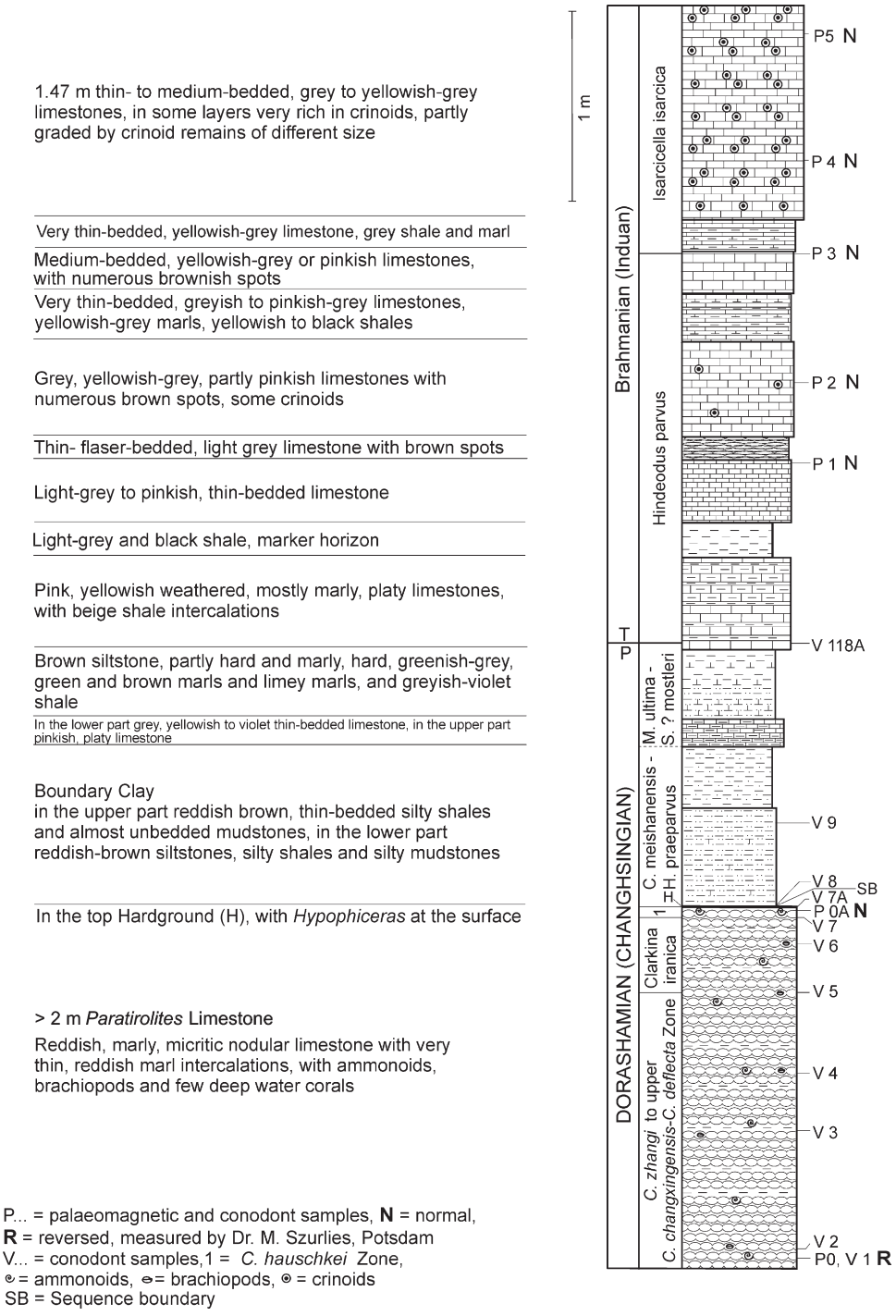

Fig. 6. Position of palaeomagnetic and important conodont samples in locality 2, section V of Kuh-e-Ali-Bashi near Jolfa, NW Iran. Modified after Szurlies and Kozur (2005).

There is a sequence boundary at the base of the Boundary Clay in all investigated sections. It is associated with a strong increase in sedimentation rate. During the time that the underlying Alibashi and upper Hambast Formations were accumulating, the sedimentation rate was very low and less than that in the contemporaneous Changxing Formation at Meishan in South China. From the base of the Boundary Clay up

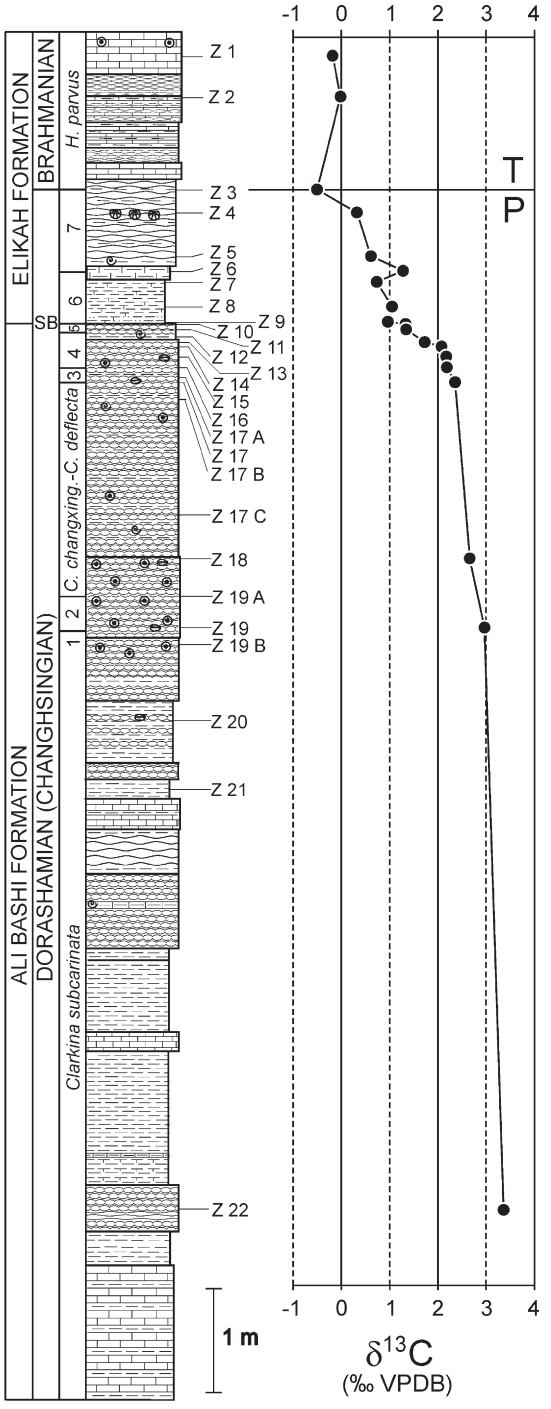

1 = *C. bachmanni* Zone, 2 = C. *nodosa* Zone,
3 = *C. zhangi* Zone, 4 = C. *iranica* Zone,
5 = *C. hauschkei Zone, 6 = C. meishanensis-praeparvus* Zone, 7 = *M. ultima - S. ? mostleri* Zone
= ammonoids = brachiopods = crinoids
= *Claraia* SB = Sequence boundary

to the *H. parvus* Zone (i.e. around the PTB) the sedimentation rate is much higher than in the contemporaneous interval at Meishan, which can be accurately correlated to the Iranian sections by conodonts. The distance from the base of the Boundary Clay to the base of the Triassic is about 0.16 m at Meishan, but 1.20–1.30 m in the investigated Iranian sections. The *H. parvus* Zone is 0.08 m at Meishan, but 1–2 m in the Iranian sections.

Wardlaw and Davydov (2005, p. 39) stated: " the correlation lines are much more expanded for Meishan for that part in common with Zal (uppermost Wuchiapingian and Changhsingian), indicating that the sedimentation rate is greater at Meishan, contrary to reports that Iranian sections are more expanded. Also, all events are consistent relative to each other and there is no missing zone or sedimentation. The new data correlate excellently with Meishan, however, when compiled with existing data reported by Kozur (written commun., 2005) it shows gaps (event correlation lines converging to a point) and inconsistencies that we are currently re-evaluating, but it appears that the ranges given by Kozur (written commun., 2005) are unreliable." The data provided by Kozur (written comm., 2005) now are published (Kozur, 2005). No one has ever published or written a personal communication stating that the upper Wuchiapingian and Changhsingian section in Iran is more expanded than in the Meishan section. This was stated and published only in regard to the sedimentation rate around the PTB, from the Boundary Clay up through the *H. parvus* Zone (see above). Kozur (2005) has stated that the sedimentation rate of the Changxing Limestone was distinctly higher at Meishan than in contemporaneous beds in the Iranian sections; it is only in the interval from the base of the Boundary Clay up to the *H. parvus* Zone that the sedimentation rate in Iran became much higher than at Meishan. It also is incorrect to state that there is no zone missing at Meishan. This will be discussed in the next paragraph (3.2. Biostratigraphy).

3.2. Biostratigraphy

The biostratigraphic zonation and dating of the Dorashamian and lowermost Triassic sections of central and northwestern Iran is discussed in detail by Kozur (2004a, 2005). It is based on detailed conodont and ammonoid zonations that can be recognised throughout the Tethys region and, in part, also into the intraplatform

Fig. 7. Lithology, conodont biostratigraphy and carbon isotope data in the middle-upper Dorashamian (middle-upper Changhsingian) and basal Triassic of the Zal section, Central Iran. Modified after Kozur (2005), carbon isotope data from Korte et al. (2004b).

basins of South China. There, some zones are not present because of endemism (typical in intraplatform basins) and possibly because there is a short time gap within the *C. iranica* Zone.

As is typical for intraplatform basins (e.g., the Middle Triassic Germanic Basin), the Changhsingian intraplatform basins in South China show a distinct endemism in their faunas. All stratigraphically important Dorashamian ammonoids of the Tethys region, some of which (the *Paratirolites* ammonoid fauna) can be traced as far away as Madagascar, are missing in the Changhsingian of South China. There, endemic genera and species replace these forms. Beginning in the *C. hauschkei* Zone, the ammonoid endemism becomes less pronounced and disappears within the low palaeolatitude deposits at the base of the Boundary Clay or a little higher. In the *C. hauschkei* Zone, the South Chinese ammonoid genus *Pleuronodoceras* invaded the Tethys region (*P. occidentale* Zakharov), and from the base of the Boundary Clay upward some ammonoids appear which can be found all the way from Greenland through the Tethys region to the Chinese intraplatform basins (*Hypophiceras*). This *Hypophiceras* fauna in Iran is restricted to the *C. meishanensis–H. praeparvus* Zone of the Boundary Clay and the *M. ultima–S.* ? *mostleri* Zone of the immediately overlying marly limestones and marls; it is gone by the *H. parvus* Zone. This confirms the Permian age of the Boreal *Otoceras boreale* Zone s.s. which includes common *Hypophiceras*. As demonstrated in Greenland (Kozur, 1998b), *H. parvus* begins in the *Tompophiceras pascoei* Zone above the *O. boreale* Zone (s.s.). The last representatives of the *O. boreale* group, however, persist up into the *T. pascoei* Zone and time equivalents (e.g., *O. fissiselatum* Diener at Selong). For this reason, the *O. boreale* Zone often has been expanded to include these forms in an *O. boreale* Zone (s.l.). This means that the *O. boreale* Zone (s.l.) straddles the PTB, though the *O. boreale* Zone (s.s.) does not.

The conodonts of South China are not so endemic as the ammonoids, but some important Dorashamian Tethyan guide forms are missing in South China or at Meishan. For example, the *C. nodosa* Zone is absent in the intraplatform basin of South China, even though that basin had water depths similar to the water depths of sections in Iran and there is no evidence for stratigraphic gaps in this part of the South China section. The conodont endemism ends in the *C. hauschkei* Zone. The absence of the *C. iranica* Zone at Meishan seems to be because of a short time gap there. Elsewhere in South China this species is present (see below).

Twelve conodont zones have been recognised by Kozur (2005) from the basal Dorashamian *C. hambastensis* Zone up to the Lower Triassic *I. isarcica* Zone (Figs. 3–8, Plates I, II). The upper Dorashamian (beginning with the *C. nodosa* Zone) to lowermost Triassic conodont zonation is very detailed and allows an exact dating of all recognised events (see Section 4). These events, in turn, can be accurately correlated with the continental uppermost Permian and lowermost Triassic in several sections of the Germanic Basin. There, Milankovitch cycles down to the ~ 20,000 years precession cycles can be readily recognised in lake deposits (Kozur, 2003, Bachmann and Kozur, 2004, Korte and Kozur, 2005, Kozur and Bachmann, 2005). This allows an estimation of the duration of these conodont zones both by marine to continental cross-correlations in Germany and by identical direct calibrations through readily recognisable Milankovitch cycles for those zones represented by shallow marine deposits in the Southern Alps (for example, the *H. parvus* Zone). These cross-correlations

Internat. scale	Tethyan Scale		Conodont Zone
Stage	Stage	Substage	
"Induan"	Brahmanian (Induan)	Gangetian	*Isarcicella isarcica*
			Hindeodus parvus
Changhsingian	Dorashamian		*Merrillina ultima - Stepanovites ? mostleri*
			Clarkina meishanensis - Hindeodus praeparvus
			Clarkina hauschkei
			Clarkina iranica
			Clarkina zhangi
			Clarkina changxingensis - Clarkina deflecta
			Clarkina nodosa
			Clarkina bachmanni
			Clarkina subcarinata
			Clarkina hambastensis

Fig. 8. Dorashamian (Changhsingian) and basal Triassic conodont zonation of Tethys.

demonstrate that the *C. zhangi* Zone is ~ 70,000 years long, the *C. iranica* Zone is ~ 60,000 years long, the *C. hauschkei* Zone is ~ 15,000 years long, the *C. meishanensis–H. praeparvus* and *M. ultima–S.* ? *mostleri* zones together are ~ 120,000 years long, the *H. parvus* Zone is ~ 100,000 years long, and the *I. isarcica* Zone is ~ 700,000 years long. Kozur (2005) documents all of these calibrations in detail. One example of this process is that the top of the *I. isarcica* Zone in the Bulla (Pufels) section of the Southern Alps, Italy, has a well studied palaeomagnetic succession (Scholger et al., 2000) that has been correlated with the top of magnetozone 1n by Bachmann and Kozur (2004). In continental beds of the Germanic Basin, Bachmann and Kozur (2004) placed this boundary at the top of magnetozone 1n.2n, which corresponds to the top of magnetozone 1n in Tethys by magnetostratigraphic correlation with the palaeomagnetic succession in the Lower Buntsandstein of the Germanic Basin (Szurlies, 2004). This level is within lithocycle 9 of the Calvörde Formation of the Germanic Buntsandstein in the cyclic subdivision of Szurlies (2004). As pointed out by Bachmann and Kozur (2004), the lithocycles of Szurlies (2004) correspond to short eccentricity cycles (~ 100,000 years), except lithocycle 4 which contains 2 short eccentricity cycles. The base of the Calvörde Fm. is the base of the Buntsandstein, marked by a sudden climate change from dry to wet. In the Tethys region, the base of the Boundary Clay is marked likewise by a climatic change indicated by the sudden disappearance of all warm water conodonts of the *C. subcarinata* lineage and their replacement by cool water conodonts (see below). This indicates that the base of the Buntsandstein correlates with the base of the Boundary Clay. This correlation can be confirmed by the equivalent position of the base of the Buntsandstein and the base of the Boundary Clay within the lower part of the long normal magnetozone that straddles the PTB, and also by the maximum abundance of cosmic microsphaerules that occurs a little above the base of both the Boundary Clay and the base of the Buntsandstein.

The base of the Triassic in continental lake deposits of the Germanic Basin lies at the boundary between the *Falsisca postera* and *F. verchojanica* conchostracan zones. This boundary can be correlated by conchostracans and sporomorphs with the marine PTB in the (marginal marine) Werfen Beds of Hungary and the Southern Alps (Kozur, 1998a,b, Bachmann and Kozur, 2004, Kozur and Bachmann, 2005). It lies one precession cycle (~ 20,000 years) above the base of lithocycle 2 of the Calvörde Fm., at the base of oolite α 2. This horizon is easily recognised in the Nelben section west of Halle in the Germanic Basin (Kozur, 2003, Bachmann and Kozur, 2004), where it is one short eccentricity cycle (lithocycle 1 sensu Szurlies, 2004) plus one precession cycle (together ~ 120,000 years) above the base of the Buntsandstein. According to the above mentioned cross-correlation with the marine realm, this uppermost Permian section corresponds to the interval from the base of the Boundary Clay (base of *C. meishanensis–H. praeparvus*) to the base of the *H. parvus* Zone. In Tethys, this interval comprises the *C. meishanensis–H. praeparvus* Zone and the *M. ultima–S.* ? *mostleri* Zone, the duration of which is (according to this cross-correlation) altogether ~ 120,000 years. The *H. parvus* Zone at the Bulla section, with its revised lower boundary (Korte and Kozur, 2005a), comprises one eccentricity cycle (~ 100,000 years). About 8.5 lithocycles (9.5 short eccentricity cycles, ~ 0.95 Myrs) are present in the interval from the base of the Buntsandstein (= base of the Boundary Clay) up to the top of the magnetozone 1n.2n (= top of the *I. isarcica* Zone, see above). This leaves somewhat more than 0.7 Myrs for the duration of the *I. isarcica* Zone (0.95 Myrs–0.12 Myrs–0.1 Myrs).

The duration of the other conodont zones mentioned above was calculated in a similar manner by a combination of palaeomagnetic and biostratigraphic correlation (Kozur, 2005). An important role is played by the very short key palaeomagnetic reversed Zone 0r that lies immediately below the long palaeomagnetic normal Zone that straddles the PTB. In the Germanic Basin, 0r comprises the lower and the basal part of the upper Fulda Formation, which represent one eccentricity cycle plus half of a precession cycle (~ 110,000 years). In Tethys, 0r comprises the upper *C. changxingensis–C. deflecta* Zone (Szurlies and Kozur, 2004) and the greater part of the *C. zhangi* Zone (conodont age established by Kozur, 2005 for this reversed Zone that was established by Zakharov and Sokarev, 1991); each conodont zone comprises about half of 0r. The normal palaeomagnetic interval from the top of 0r to the base of the Buntsandstein (corresponding to the base of the Boundary Clay, see above) comprises in the Germanic Basin somewhat less than one eccentricity cycle (~ 90,000 years). In the Iranian sections and at Dorasham 2 (Zakharov and Sokarev, 1991) this interval corresponds to the uppermost *C. zhangi* (from the base of its upper quarter), the *C. iranica*, and the *C. hauschkei* Zones with a ratio of 1:4:1 for the three zones. Under the assumption that the sedimentation rates in these very short zones in deeper water environments was nearly constant, the duration of these 3 conodont zones (see above) can be estimated. No detailed cross-correlation is possible for the *C. nodosa* and *C. changxingensis–C. deflecta* Zones, but comparing the thickness of the two overlying zones in unreduced sections,

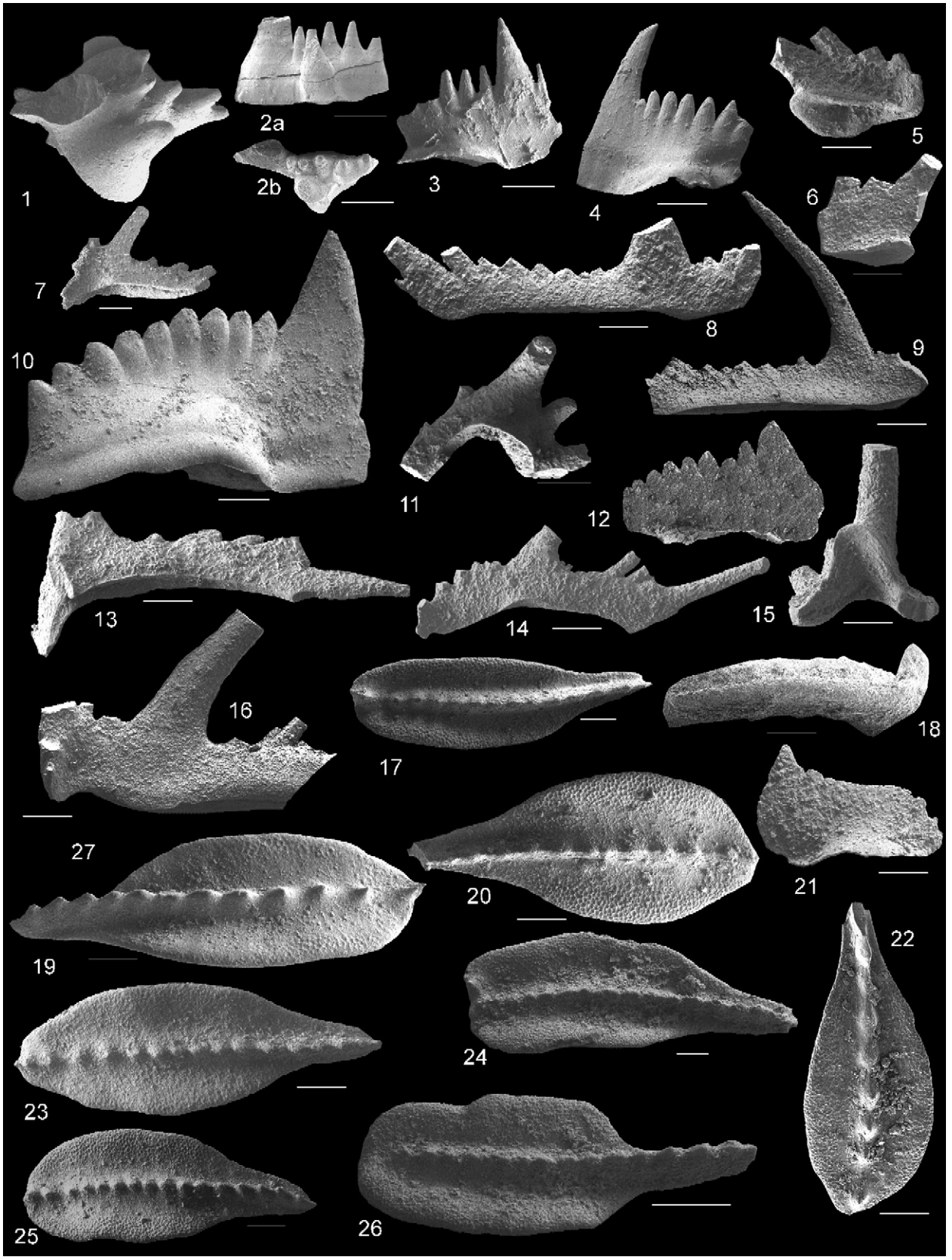
1
2a
2b
3
4
5
6
7
8
9
10
11
12
13
14
15
16
17
18
19
20
21
22
23
24
25
26
27

under an assumption of constant sedimentation rate for the deeper water sediments, the *C. nodosa* Zone should be about as long as the *C. iranica* Zone or a little less (~ 50,000 to 60,000 years) and the *C. changxingensis–C. deflecta* Zone is about as long as the *C. zhangi* and *C. iranica* Zones together (~ 130,000 years).

The unusually short duration of all conodont zones in the interval from the *C. nodosa* up to the *H. parvus* Zone indicates high ecological stress. The extremely short *C. hauschkei* Zone is the uppermost zone with warm water conodonts, and it terminates with the extinction event for warm water conodont faunas at the base of the Boundary Clay. In the Abadeh sections, situated about 7° north of the Tropic of Capricorn in the Permian southern hemisphere (Stampfli and Borel, 2004), only a depauperate cool water conodont fauna with *Hindeodus*, e.g. *H. altus* Kozur, Plate II, Fig. 1, and *Merrillina* is present in the *C. hauschkei* Zone. *Merrillina* is a cool water genus according to Mei Shilong and Henderson (2001) whereas *Hindeodus* is common in (but not restricted to) cool water. In more northerly sections, closer to the equator at that time, the depauperate cool water fauna does not appear until the base of the *C. meishanensis–H. praeparvus* Zone, for example around the palaeo-equator (Sicily) and a little north of it (South China).

In Iran, the *C. zhangi* Zone (introduced by Wardlaw, 2004, instead of the *C. yini–C. zhangi* Zone, and adopted by Kozur, 2005, because Mei Shilong, the author of *C. yini* Mei, reported in Sweet and Mei (1999a,b) that this form at Jolfa ranged down to the level of the *C. bachmanni* Zone), *C. meishanensis–H. praeparvus* Zone, *H. parvus* Zone and *I. isarcica* Zone can be directly correlated with the same conodont zones in South China. The *M. ultima–S.* ? *mostleri* Zone can be accurately correlated with the *C. zhejiangensis* Zone at Meishan. The *C. changxingensis–C. deflecta* Zone (introduced by Wang and Wang, 1981), can be roughly correlated with the zone of the same name at Meishan. In South China, *C. nodosa* is missing due to endemism (see above). Therefore, the time interval of the *C. nodosa* Zone in Iran must be included in the *C. changxingensis–C. deflecta*

Plate I. Scale = 100 μm. Fig. 1. *Isarcicella isarcica isarcica* (Huckriede), Pa element, upper view, Jolfa, Kuh-e-Ali Bashi, locality 2, section V, sample JV-P 4, *I. isarcica* Zone, Gangetian, Brahmanian (Induan), rep.-no. 2003-6/VII-115. Fig. 2. *Isarcicella isarcica staeschei* (Dai and Zhang), Pa element, Abadeh, Kuh-e-Hambast, section VI, sample Aba 72, lowermost *I. isarcica* Zone, lower Gangetian, Brahmanian (Induan), rep.-no. 2000/II-86, a) lateral view, b) upper view. Fig. 3. *Hindeodus parvus anterodentatus* (Dai, Tian and Zhang), Pa element, lateral view, Zal section I, sample Zal 1, lower Elikah Fm., upper *H. parvus* Zone, lower Gangetian, Brahmanian (Induan), rep.-no. 2003-6/III-5. Fig. 4. *Hindeodus parvus* (Kozur and Pjatakova), Pa element, lateral view, Zal section I, sample Zal 1, lower Elikah Fm., upper *H. parvus* Zone, lower Gangetian, Brahmanian (Induan), rep.-no. 2003-6/III-1. Figs. 5–9, 11, 13, 14. *Merrillina ultima* Kozur, lower Elikah Fm., *M. ultima–S.* ? *mostleri* Zone, uppermost Dorashamian; Figs. 5, 6, 8, 9, 13, 14: Zal section I, sample Zal 5; Fig. 7: Shahreza section, sample Sh 71A; Fig. 11: Shahreza section, sample Sh 70; Figs. 5, 6: Pa element, lateral view; Fig. 5: rep.-no. 2003-6/III-50; Fig. 6: rep.-no. 2003-6/III-52; Fig. 7: Pb element, rep.-no. 2003-6/VII-31; Figs. 8, 9: Sc element; Fig. 8: rep.-no. 2003-6/III-54; Fig. 9: rep.-no. 2003-6/III-47; Fig. 11: M element; rep.-no. 2003-6/I-56; Fig. 13: Sa element, rep.-no. 2003-6/III-51; Fig. 14: Sb element, rep.-no. 2003-6/III-67. Fig. 10. *Hindeodus magnus* Kozur, lateral view, Zal section I, sample Zal 3, lower Elikah Fm., base of *H. parvus* Zone, base of Gangetian, base of Brahmanian (Induan), rep.-no. 2003-6/III-16. Fig. 12. *Hindeodus praeparvus* Kozur, Pa element, lateral view, Kuh-e-Hambast, 60 km SE of Abadeh, section V, sample Aba V-3, lowermost Elikah Fm., 1 cm limestone bed within the upper 7 cm of the Boundary Clay, *C. meishanensis–H. praeparvus* Zone, uppermost Dorashamian, rep.-no. 2003-6/VII-73. Figs. 15, 16. *Stepanovites* ? *mostleri* Kozur, Zal section I, sample Zal 5, lower Elikah Fm., *M. ultima–S.* ? *mostleri* Zone, uppermost Dorashamian; Fig. 15: M element, rep.-no. 2003-6/III-39; Fig. 16: Sc element; rep.-no. 2003-6/III-63. Fig. 17. *Clarkina meishanensis* Zhang, Lai, Ding and Liu, Pa element, upper view, Zal, section 1, sample Zal 11, uppermost Alibashi Fm. above the *Paratirolites* Limestones, 4–9 cm below the Boundary Clay, *C. hauschkei* Zone, upper Dorashamian, rep.-no. 2003-6/III-92. Fig. 18. *Clarkina meishanensis* Zhang, Lai, Ding and Liu, Pa element, lateral view, Shahreza section, sample Sh 60, uppermost Hambast Fm., uppermost Unit 7, 4–6 cm below the Boundary Clay, *C. hauschkei* Zone, upper Dorashamian, rep.-no. 2000/II-8. Fig. 19. *Clarkina hauschkei* Kozur, Pa element, upper view, Jolfa section, Kuh-e-Ali Bashi, locality 2, section V, sample J V-7A, top of Alibashi Fm., *C. hauschkei* Zone, upper Dorashamian, rep.-no. 2003-6/VII-89. Fig. 20. *Clarkina hauschkei borealis* Kozur, Pa element, upper view, in the big gap between the cusp and the last denticle of the carina is a matrix grain which looks like an additional denticle, Shahreza section, sample Sh 62, uppermost Hambast Fm., top of Unit 7 (uppermost 2 cm below the Boundary Clay), *C. hauschkei* Zone, upper Dorashamian, rep.-no. 2003-6/VII-3. Fig. 21. *Hindeodus changxingensis* Wang, Pa element, lateral view, sample Aba V-3 (see Fig. 20), rep.-no. 2003-6/VII-76. Fig. 22. *Clarkina hauschkei borealis* Kozur, Pa element, upper view, sample KD-2, locality 6.75 according to Teichert and Kummel (1976), Kap Stosch, East Greenland, basal Wordie Creek Fm., basal *Otoceras* Beds (basal *Hypophiceras triviale* Zone, equivalent of basal *O. boreale* Zone), *C. hauschkei* Zone, uppermost Permian, rep.-no. 23-6-96/VI-23. Fig. 23. *Clarkina nassichuki* Orchard, Pa element, upper view, Shahreza section, sample Sh 62A, uppermost Hambast Fm., 2–4 cm below the top of Unit 7, *C. hauschkei* Zone, upper Dorashamian, rep.-no 2003-6/VI-39. Fig. 24. *Clarkina tulongensis* (Tian), upper view, Zal, section 1, sample Zal 10, uppermost Alibashi Fm. above the *Paratirolites* Limestone, 2–3 cm below the Boundary Clay, *C. hauschkei* Zone, upper Dorashamian, rep.-no. 2003-6/III-75. Fig. 25. *Clarkina praetaylorae* Kozur, upper view, Shahreza section, sample Sh 62A, uppermost Hambast Fm., 2–4 cm below the top of Unit 7, *C. hauschkei* Zone, upper Dorashamian, rep.-no. 2003-6/VII-38. Fig. 26. *Clarkina iranica* Kozur, upper view, Zal, section I, sample Zal 13, uppermost Alibashi Fm., upper *Paratirolites* Limestone, 0.2 m below the Boundary Clay, upper *C. iranica* Zone, upper Dorashamian, rep.-no. 2003-6/III-103.

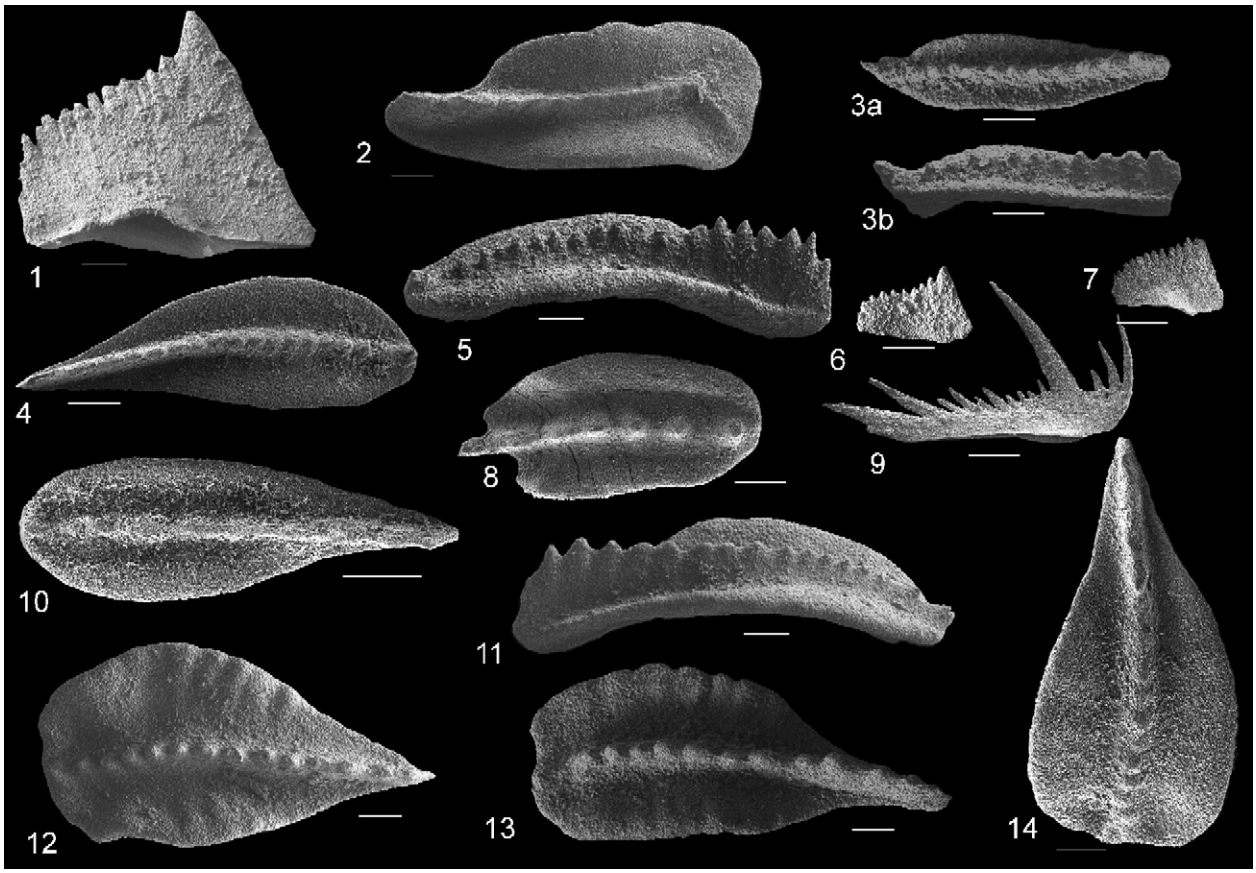

Plate II. Scale=100 μm. Fig. 1. *Hindeodus altus* Kozur, Pa element, holotype, Abadeh, Kuh-e-Hambast, section I, sample Aba I NA5, 5–8 cm below the top of Unit 7 of the uppermost Hambast Fm., cool water fauna of the *C. hauschkei* Zone, upper Dorashamian, rep.-no. 2003-6/VIII-9. Fig. 2. *Clarkina abadehensis* Kozur, upper view, Jolfa, Kuh-e-Ali Bashi, locality 1, section III with strongly reduced *C. iranica* Zone, sample J 102, uppermost Alibashi Fm., upper *Paratirolites* Limestone, 5 cm below the Boundary Clay, rep.-no. 9-3-01/IV-10. Fig. 3. *Clarkina zhangi* Mei, Shahreza section, sample Sh 54, uppermost Hambast Fm., upper unit 7 at 64 cm below the Boundary Clay, *C. zhangi* Zone, upper Dorashamian, rep.-no.2003-6/II-1, a) upper view, b) lateral view. Fig. 4. *Clarkina yini* Mei, upper view, Jolfa, Kuh-e-Ali Bashi, locality 1, section III with strongly reduced *C. iranica* Zone, sample J 101, uppermost Alibashi Fm., upper *Paratirolites* Limestone, 10 cm below the Boundary Clay, *C. zhangi* Zone, upper Dorashamian, rep.-no. 9-3-01/III-24. Fig. 5. *Clarkina yini* Mei, lateral view, Shahreza section, sample Sh 54A, upper Unit 7 of uppermost Hambast Fm., 0.50 m below the Boundary Clay, *C. yini–C. zhangi* Zone, upper Dorashamian, rep.-no. 2003-6/VI-69. Fig. 6,7. *Hindeodus typicalis* (Sweet), small forms, Pa element lateral view; Fig. 6: Shahreza section, sample Sh 53, upper Hambast Fm., upper unit 7 at 0.75 cm below the Boundary Clay, cool water fauna from the lower *C. yini–C. zhangi* Zone, rep.-no.2003-6/I-73; Fig. 7: Abadeh, Kuh-e-Hambast, section VI, sample Aba 53, upper Hambast Fm., upper Unit 7 at 0.93 m below the Boundary Clay, cool water fauna of the *C. yini–C. zhangi* Zone, upper Dorashamian, rep.-no. 9-3-01/VI-31. Fig. 8. *Clarkina* n. sp. B of *C. carinata* group, very wide spaces between the denticles of the carina, as typical for Permian cool water gondolellids, upper view, Abadeh, Kuh-e-Hambast, section VI, sample Aba 53, upper Hambast Fm., upper Unit 7 at 0.93 m below the Boundary Clay, cool water fauna of the *C. zhangi* Zone, upper Dorashamian, rep.-no. 9-3-01/VI-27. Fig. 9. *Merrillina* sp. of *M. divergens* group, Sc element, Jolfa, Kuh-e-Ali Bashi, locality 1, section III with strongly reduced *C. iranica* Zone, sample J 99, uppermost Alibashi Fm., upper *Paratirolites* Limestone, 0.5 m below the Boundary Clay, cool water fauna of the *C. yini–C. zhangi* Zone, upper Dorashamian, rep.-no. 9-3-01/III-14. Fig. 10. *Clarkina changxingensis* (Wang and Wang), upper view, Jolfa, Kuh-e-Ali Bashi, locality 1, section III, sample J 96, uppermost Alibashi Fm., upper *Paratirolites* Limestone, 1.2 m below the Boundary Clay, rep.-no. 9-3-01/III-2. Fig. 11. *Clarkina changxingensis* (Wang and Wang), lateral view, sample Sh 54A (see Fig. 5), rep.-no. 2003-6/VI-72. Figs. 12, 13. *Clarkina nodosa* Kozur, upper view, Zal section I, sample Zal 19, upper Alibashi Fm., lower *Paratirolites* Limestone, 3 m below the Boundary Clay, *C. nodosa* Zone, upper Dorashamian; Fig. 12: rep.-no. 2003-6-/IV-52; Fig. 13: rep.-no. 2003-6-/IV-51. Fig. 14. *Clarkina deflecta* (Wang and Wang), upper view; Kuh-e-Ali Bashi, locality 1, section III with strongly reduced *C. iranica* Zone, sample J 95, uppermost Alibashi Fm., middle *Paratirolites* Limestone, 1.4 m below the Boundary Clay, C. *changxingensis–C. deflecta* Zone s.s., upper Dorashamian, rep.-no. 9-3-01/II-24.

Zone at Meishan, so that the *C. changxingensis–C. deflecta* Zone begins earlier at Meishan than in Iran.

Wardlaw (in Wardlaw and Davydov, lecture in Albuquerque, October 2005) placed a newly defined *C. deflecta* Zone above the *C. zhangi* Zone at Meishan. In such a position, his *C. deflecta* Zone at Meishan does not correlate with the Tethys region. Probably Wardlaw's *C. deflecta* Zone is based on *C. tulongensis* (Tian), which is common above the *C. zhangi* Zone (especially in the *C. hauschkei* Zone) and often consists of forms that have deflected posterior carina. These forms sometimes have been assigned incorrectly to *C. deflecta* (Wang and Wang). The (*C. yini*–) *C. zhangi* Zone occurs at Meishan from about 0.8 m to 0.1 m below the top of the Changxing Limestone (Mei Shilong et al., 1998), and neither index species is present lower than 0.80 m below the top of the Changxing Limestone at Meishan. The holotype of *C. deflecta* (Wang and Wang) was found 7.40 m below the top of the Changxing Limestone. The other specimen illustrated by Wang and Wang (1981) was found 2.97 m below the top of the Changxing Limestone (both specimen horizons were provided to me by Prof. Wang-Chengyuan, Nanjing, one of the describers of *C. deflecta*). Thus, both of the originally illustrated specimens of *C. deflecta* were found far below the base of the *C. zhangi* Zone, and they clearly are different from the forms above the *C. zhangi* Zone that have a deflected carina (*C. tulongensis*). Specimens of *C. deflecta* that correspond to the holotype do not occur above the *C. zhangi* Zone. It is also important to note that the deflected posterior end of the carina is not a species-diagnostic feature; it occurs in a number of Permian and Triassic gondolellids.

Most probably, the *C. deflecta* Zone above the *C. zhangi* Zone at Meishan (sensu, in Wardlaw and Davydov, lecture in Albuquerque October 2005) corresponds to the *C. hauschkei* Zone. This is indicated by its position immediately below the Boundary Clay. Wardlaw has reported *C. hauschkei* from the uppermost 2 cm of the Changxing Limestone at Meishan (pers. comm., Albuquerque 2005, though he did not have photographs there of this species), so it seems likely that the nearly cosmopolitan *C. hauschkei* Zone also is present at Meishan.

The *C. hauschkei* Zone can be correlated as far away from the Tethys region as Greenland (Kozur, 2004a), where *C. hauschkei borealis* Kozur, which is also present in Iran (Plate I, Fig. 20), occurs in the lower *Hypophiceras triviale* Zone of Greenland (Plate I, Fig. 22). This zone is an equivalent of the lowermost *O. boreale* Zone (Kozur, 1998a,b, 2004a, 2005). Moreover, *C. hauschkei* also is present in the lower *O. boreale* Zone of Arctic Canada (= *C.* cf. *subcarinata* (s.l.) sensu Henderson and Baud, 1997; see Kozur, 2004a). The *C. hauschkei* Zone also is present in the lowermost 4 cm of the *Otoceras* Beds at Guling, Spiti. There it occurs in brownish, soft iron oxides that for a long time were regarded as evidence of subaerial weathering on the top of the underlying Guling Shales. During an excursion in the summer of 2004, however, a new outcrop was found in which these soft iron oxides grade laterally into limestones (with xenodiscid ammonoids) at the base of the *Otoceras* Beds.

The *C. meishanensis–H. praeparvus* and *H. parvus* Zones can be correlated directly with the same zones in the Boreal realm, also at the margin of Gondwana in the Salt Range, and in Guling (Spiti) based on my personal unpublished material.

There are no known occurrences in situ of *C. iranica* Kozur in South China, but it does occur in the Xifanli section in Daye County, southeast Hubei Province. There, numerous *C. iranica* and *C. abadehensis* were illustrated from the *C. meishanensis–H. praeparvus* Zone by Lai Xulong et al. (1999), who erroneously assigned these forms to *C. meishanensis* Zhang, Lai, Ding and Liu and *C. deflecta* and also erroneously assigned real *C. meishanensis* to *C. carinata* (Clark). The numerous reworked specimens of *C. iranica* and *C. abadehensis* in the Boundary Clay of this section indicate that sediments of the *C. iranica* Zone had been deposited there at one time. These sediments may have been removed by the high-energy event at the base of the Boundary Clay, as is the case locally in the Iranian sections. These rich occurrences are important, because they show that *C. iranica* was not absent in South China because of endemism.

The absence of *C. nodosa*, *C. abadehensis*, and *C. iranica* at Meishan cannot be explained as a result of any difference in facies. These species are the most common forms in the Dorashamian of the Tethys region. They occur (sometimes together with *C. sosioensis* Gullo and Kozur of the *C. iranica* group, which is more common in equatorial areas like Sicily) in diverse facies from red deep-sea clays through red and dark grey deep water limestones to moderately deep water limestones deposited above the storm wave base. Meishan falls within this range of facies in which *C. iranica* occurs. Although Wardlaw (2004) reported *C. abadehensis* from Meishan (without illustration) in material supplied by C. Henderson (Calgary), C. Henderson (pers. comm.) denies the presence of any form similar to *C. abadehensis* in his material. Thus both *C. abadehensis* and *C. iranica* appear to be absent at Meishan (despite a rich occurrence at the Xifanli section in South China, see above). Their absence can be explained neither by endemism nor by facies-controlled depositional setting, so

this seems to indicate that there must be a short depositional and time gap in the Meishan section at the level of the *C. iranica* Zone.

Within three stratigraphic intervals below the Boundary Clay (within the upper *C. subcarinata* Zone, within the middle *C. changxingensis–C. deflecta* Zone, and in the lower *C. zhangi* Zone) the Dorashamian warm water conodont faunas disappear and are replaced by a cool water fauna with small *H. typicalis* (Plate II, Figs. 6–7) and a few *Merrillina* sp. (Plate II, Fig. 9). Occasionally a *Clarkina* n. sp. (Plate II, Fig. 8) is present which is not part of the Dorashamian warm water conodont faunas. This form has very widely spaced denticles on its carina. According to C. Henderson (lecture in Albuquerque, October 2005), this feature is typically found on Permian cool water gondolellids.

The uppermost cool water interval below the Boundary Clay in the lower *C. zhangi* Zone is especially obvious. The basal part of the *C. zhangi* Zone and the upper *C. zhangi* Zone contain an identical warm water conodont fauna, but this totally disappears in the intervening cool water portion of the lower *C. zhangi* Zone. This cool water interval can be accurately correlated with continental beds by the presence of a short reversed interval (0r according to Bachmann and Kozur, 2004, Kozur and Bachmann, 2005), which comprises the upper *C. changxingensis–C. deflecta* Zone and most of the *C. zhangi* Zone. On the Russian Platform, this reversed interval corresponds o the Nedubrovo Formation. There, in the upper part of 0r, a fallout of mafic tuffs is present (Lozovsky et al., 2001) that originated about 3000 km away in the eruption centres of the Siberian Trap in the Tungusska Basin. Both in the Germanic Basin (upper 0r in the upper part of lower Fulda Formation and lowermost upper Fulda Fm.) and in Iran (upper 0r in the lower *C. zhangi* Zone) this horizon contains volcanic microsphaerules. Thus, a direct correlation can be made between the timing of this immigration of a cool water fauna into the tropical realm and an especially strong interval of explosive volcanic activity that was taking place during the Siberian Trap episode. During this time, cool water conodont faunas immigrated northwards to an area between about 7° north of the Permian Tropic of Capricorn in central Iran (Abadeh area) to more than 1000 km north of this palaeolatitude (Jolfa, Zal sections and Transcaucasian sections, such as Dorasham 2, Achura, Sovetashen). The displaced warm water conodont fauna retreated to the inner tropical (equatorial) realm. When volcanic activity ceased and oceanic water temperatures rose, the warm water faunas spread north and south again, unchanged or nearly unchanged as seen in the upper *C. zhangi* Zone. At the base of the Boundary Clay, a total replacement of the warm water conodont fauna by a depauperate cool water fauna is seen again. This fauna contains mostly small *Hindeodus*, a few *Merrillina*, *C. meishanensis*, and rare *C. taylorae* (Orchard). Although *C. taylorae* is very rare in the low latitude Iranian sections, it is very common in areas that were in higher northern and southern palaeolatitudes. This cooling event culminated in the *M. ultima–S.* ? *mostleri* Zone, in which the cool water genus *Merrillina* is the dominant element in the Iranian conodont faunas.

In the cases discussed above, the warm water conodont faunas in the Tethys region were replaced completely by cool water faunas, but this did not happen in the equatorial inner tropical belt. As a result, the warm water fauna was able to spread back across the Tethys region each time that the climate warmed again. At the base of the Boundary Clay, however, this replacement took place also throughout the equatorial inner tropical belt (e.g., Sosio and South China, situated around and a little north of the palaeo-equator). This meant that there was no longer a tropical refugium in which the warm water fauna could survive, and so it went extinct. It may be that in this event there was an added stress due to the influence of a bolide impact, but the maximum abundance of cosmic microsphaerules lies a little above the base of the Boundary Clay so the correlation is not very precise. Also, in the *C. hauschkei* Zone, a gradual cooling can be observed before the warm water conodont fauna is totally replaced by a cool water conodont fauna. This replacement started earlier (at the base of the *C. hauschkei* Zone) in regions farther away from the palaeo-equator (e.g., the Abadeh area somewhat north of Tropic of Capricorn) than it did in more equatorial areas that lay more than 1000 km to the north (Jolfa, Zal and Transcaucasian sections). In these latter areas, the warm water fauna gradually disappeared within the *C. hauschkei* Zone and is partly replaced by immigrants from the cool water faunas from the Gondwana margin, e.g., *C. kazi* (Orchard), *C. meishanensis* (Plate I, Figs. 17, 18), *C. nassichuki* (Orchard) (Plate I, Fig. 23), *C. praetaylorae* Kozur (Plate I, Fig. 25) and *C. tulongensis* (Plate I, Fig. 24).

The identical pattern of extinction that occurs both at the base of the cool water horizon in the lower half of the *C. zhangi* Zone and at the base of the Boundary Clay, argues that they both resulted from very similar causes. Kozur (1998a,b) assumed that the mass extinction close to the PTB resulted from a volcanic winter that occurred due to the combined effects of a huge explosive felsic to intermediate volcanic event in the low northern palaeolatitudes of South China (previously regarded by Yin et al., 1992 as an important cause for the mass

extinctions close to the PTB) and the Siberian Trap volcanism. In low latitudes, the cooling by the volcanic winter and the blocking of sunlight together were the major causes of mass extinction. In high northern latitudes, the blocking of sunlight was the major factor. Both of these huge volcanic centres, which generated fallout over an area of at least 2 million km^2, were in the northern hemisphere at both low and high latitudes. In contrast, the convergent volcanism along the Gondwana margin (Veevers et al., 1994) was not accompanied with such huge areas of fallout. No major extinction event (or only a minor extinction event) therefore would be expected at high southern palaeolatitudes if the two volcanic centres in the low and high northern palaeolatitudes were the main reason for the extinctions there. This has been verified recently by Takemura et al. (2003) and Yamakita et al. (2003). They found a continuous radiolarite succession of latest Permian and earliest Triassic age at Arrow Rocks in the Waipapa Terrane, Northern Island, New Zealand. In low palaeolatitudes, including the Panthalassa Ocean, and at high northern latitudes there is a radiolarite gap that starts in the *C. hauschkei* Zone and ends only in the Upper Olenekian (Spathian). During this time interval, very few radiolarians are known from low palaeolatitudes. In contrast, at Arrow Rocks all major Permian radiolarian groups (Ruzhencevispongacea, diverse Entactinaria, and a few Albaillellaria) survive across the PTB, and the Permian forms only later disappear successively during the Gandarian (upper Brahmanian = upper Induan) and Smithian (lower Olenekian) intervals. My re-study of the conodonts and radiolarians of the Upper Permian – Lower Triassic radiolarites of Arrow Rocks confirmed all data of the above mentioned authors (conodont-rich Brahmanian = Induan radiolarites above the Permian radiolarites, no Lower Triassic radiolarite gap, no mass extinction close to the PTB).

3.3. Events in the upper dorashamian and lowermost triassic in central and NW Iran

The following events have been observed in the upper Dorashamian and lowermost Triassic in the investigated sections:

(1) A continuous drop of $\delta^{13}C_{carb}$ occurs (Figs. 4, 7 for Shahreza and Zal sections (Korte and Kozur, 2005a; Korte et al., 2004a,b,c). Initial values around 3‰ in the *C. nodosa* Zone decline to values slightly below 0‰ by the base of the *H. parvus* Zone. After a short recovery in the upper *H. parvus* Zone, often a second negative excursion occurs in the lower *I. isarcica* Zone (see Korte et al., 2004b, Fig. 1 for Shahreza). Within the interval of nearly continuous drop of $\delta^{13}C_{carb}$, from the *C. nodosa* Zone up to the base of the Triassic, only a short recovery to values at most around 2‰ occurred in the uppermost *C. meishanensis–H. praeparvus* Zone (Figs. 4,7). The strong and abrupt negative excursion in the Boundary Clay of Meishan is only a secondary signal that also occurs in Iran. This signal occurs only when weathered Boundary Clay with very low carbonate content is investigated, as at Meishan, Abadeh, and Jolfa (Korte et al., 2004a, Korte and Kozur, 2005a). If unweathered Boundary Clay is investigated, as in Shahreza and Zal in Iran (Figs. 4, 7, Korte et al., 2004b,c) and Gerennavár in the Bükk Mountains of Hungary (Korte and Kozur, 2005a), this negative excursion is not seen. It is also absent in shallow water sections, where the Boundary Clay is replaced by marls and sometimes limestones (Korte and Kozur, 2005a). It seems significant that the interval that shows the strongest ecological stress, as indicated by the very short conodont zones, coincides with the interval of continuous drop in $\delta^{13}C_{carb}$.

(2) A short reversed palaeomagnetic zone is recognised (duration according to cross-correlation with continental beds of ~ 110,000 years) that occurs in the upper *C. changxingensis–C. deflecta* Zone and in the greater part of the *C. zhangi* Zone (Fig. 9, magnetozone 0r, Kozur, 2004b, Szurlies, 2004, Szurlies and Kozur, 2004, Bachmann and Kozur, 2004, Kozur and Bachmann, 2005).

(3) A sudden facies change occurs at the base of the Boundary Clay. This change is accompanied by a significant extinction event within the warm water fauna (related to a strong climatic change) that did not greatly affect the eurytherm benthos (small foraminifers, ostracods). Whereas the base of the Boundary Clay represents a synchronous event that caused a rapid drop in biogenic carbonate production (most probably caused by blocked sunlight), the extinction of the warm water faunas is diachronous. The extinction event occurs at the base of the *C. hauschkei* Zone slightly north of the Tropic of Capricorn (Abadeh section), but not until the base of the *C. meishanensis–H. praeaeparvus* Zone 1000 km closer to the palaeo-equator (Jolfa, Zal sections) and at the palaeo-equator itself or a little north of it (Sosio Valley of western Sicily, Italy, and South China).

(4) A strong climatic change also can be documented at the base of the Boundary Clay (see 3).

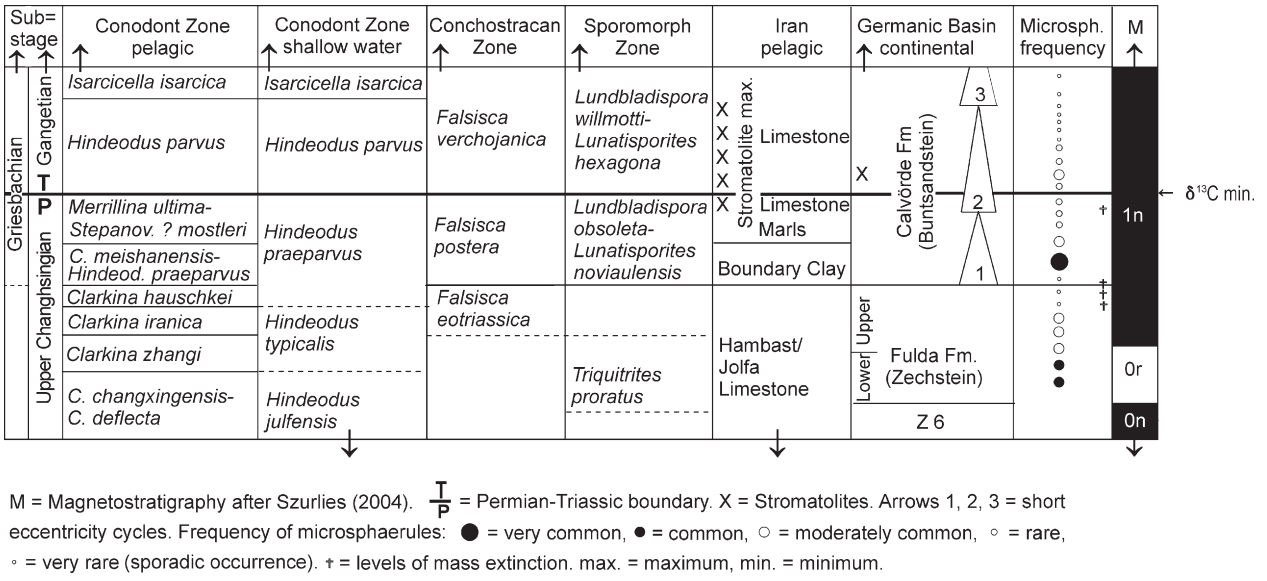

Fig. 9. Conodont, conchostracan and sporomorph zonations around the PTB in Iran and Germany. Modified after Bachmann and Kozur (2004). Not to scale.

(5) A high-energy event occurred at the base of the Boundary Clay, which also can be seen in the Bükk Mountains several thousand kilometres away. This event probably is related to huge tsunamies. This high-energy event was first recognised at Gerennavár in the Bükk Mountains, at the base of the only well-dated Boundary Clay section that formed in a shallow water environment (Kozur, 1988). There, the lower Boundary Clay contains not only numerous clasts from underlying strata, but also clasts of whitish stromatolitic limestone that were derived from rocks that occur only 50 km or more from this site. The abundant silt and occasional quartz grains in the Boundary Clay at Gerennavár also are unusual for this area, because the underlying Lopingian Nagyvisnyó Formation consists of limestone with intercalations of shale and the overlying Gerennavár Formation consists of limestone. Any possible sources of silt or sand grains (coastal or continental areas) are more than 100 km away. In the Iranian sections, only a few centimetres of reworked soft sediment occur, though locally the several centimetre-thick *C. hauschkei* Zone (and sometimes also the upper part of the underlying *C. iranica* Zone) are removed and their conodonts reworked into sedimentary pockets at the base of the Boundary Clay. In the Iranian sections, this is very curious because, in all sections, the upper Dorashamian below the *C. hauschkei* Zone consists of pink to reddish pelagic limestones with a few thin shales that were deposited below the storm wave base. The Abadeh sections are the shallowest, but even there the deposition in this interval was below the storm wave base (Fig. 3). In the Boundary Clay there is an initial shallowing, but only the immediately overlying beds with thick thrombolites are shallow water limestones and marls. Ostracods from below the shallow-water beds of the *M. ultima–S. ? mostleri* Zone mainly are bairdiaceans (without *Acanthoscapha*) and species of bythoytheracea are absent. On the other hand, typical shallow water ostracods, such as species of Kirkbyacea and Hollinellacea, also are absent or very rare. The complexion of this fauna indicates a water depth between 50 and 80 m (Fig. 3). In the Jolfa and Zal sections, the upper Dorashamian beds below the Boundary Clay occasionally contain a few *Acanthoscapha* and species of Bythcytheracea together with dominantly smooth species of Bairdiacea. For these beds, a water depth of 100–150 m is indicated. Although a shallowing trend occurred within the Boundary Clay, the water depth remained below the storm wave base at about 50–80 m water depth. Yet even here, the high-energy event is recognisable. At the Zal section, with the greatest water depth among the investigated sections, small clasts of the underlying greenish-grey marls (0.5 to 3 mm in size) can be found in the lowermost 2–3 cm of the reddish-brown Boundary Clay.

(6) Rapid but stepwise extinctions occurred among the eurytherm benthos in the interval from the base of the *M. ultima–S.* ? *mostleri* Zone up to the very base of the *H. parvus* Zone. These extinctions occur earlier in the southern sections than they do in the more northerly sections closer to the Permian palaeo-equator.
(7) A maximum development of microbialites (including large stromatolite or thrombolite bodies in shallower sections) occurs in the *H. parvus* Zone. This culminates a trend that began earlier in the *M. ultima–S.* ? *mostleri* Zone.
(8) There is an approximately 300,000 year-long interval (*C. zhangi* Zone to lower *H. parvus* Zone) during which microsphaerules are unusually abundant. The first maximum of mostly volcanic microsphaerules in the lower *C. zhangi* Zone coincides with the third cool water interval. A second and strongest maximum (cosmic and volcanic microsphaerules) occurs in the lower (but not lowermost) Boundary Clay.

Except for event 6, all events can be traced into other marine sections including the well-studied section at Meishan (e.g., Yin and Zhang, 1996; Yin et al., 1996a,b, 2001; Jin et al., 2000 and references in these papers). These events, except 5 and 6, also are readily recognisable in continental sections, such as in the Germanic Basin (Fig. 9, Kozur, 2003; Bachmann and Kozur, 2004; Kozur and Bachmann, 2005).

It is especially important that the PTB in the investigated Iranian sections lies in red sediments or, if it lies in light grey sediments as in Abadeh, the contained ostracod fauna includes species of bairdiids, cytherocopids, and kirkbyids that indicate high oxygen content in the bottom water. These ostracod groups could not live under conditions with reduced oxygen or even under dysaerobic conditions. Therefore, anoxia cannot be the ultimate reason for the PTB extinction because this occurs only locally or sometimes regionally as an overprint on the extinction event. In many areas (the Palaeotethys and low latitude Panthalassa), anoxic or dysaerobic conditions did start around the base of the Boundary Clay. In these cases, the extinction of the benthos does coincide with the extinction of the warm water conodont fauna at the base of the Boundary Clay. In these dysaerobic beds, the ostracod fauna of the Boundary Clay and the basal Triassic consists of a very few but common species, namely *H. tingi* (Patte), *Cavellina* ? sp., and, in the *C. meishanensis–H. praeparvus* and *M. ultima–S.* ? *mostleri* Zone, *Indivisia buekkensis* Kozur and *I. symmetrica* Kozur (Kozur, 1985a,b) as well. These are all filter feeders that could live under dysaerobic conditions. This ostracod fauna indicates that dysaerobic conditions existed even in sediments that now are light grey laminated marly limestones, such as the South Alpine Mazzin Member. In contrast, oxygen-rich bottom waters are indicated for the Boundary Clay and the immediately overlying beds of the *M. ultima–S.* ? *mostleri* Zone in Iran, because their ostracod faunas consist of species of bairdiids, cytherocopids, and a few kirkbyids, which in the Boundary Clay are almost as diverse as in underlying beds. In the *M. ultima–S.* ? *mostleri* Zone, however, diversity declines upward into the lowermost Triassic until only very low-diversity faunas remain. Even here, however, oxygen-rich bottom waters are indicated because the filter feeders that dominate the dysaerobic faunas are absent. This depauperate Iranian fauna is dominated by *Praezabythocypris ottomanensis* (Crasquin–Soleau), which also dominates in the Gangetian. In the *M. ultima–S.* ? *mostleri* Zone and the very base of the *H. parvus* Zone, the disaster species *Praezabythocypris pustulosus* Kozur and Mette n. sp. is very common (this is the only sculptured *Praezabythocypris* species). Also, conodont disaster species occur in this same short interval, indicating very high ecological stress (e.g. *Hindeodus changxingensis* Wang, Plate I, Fig. 21, and the very big *Hindeodus magnus* Kozur, Plate I, Fig. 10). The significant extinction event at the base of the Boundary Clay affected both warm water nekton and the entire benthos only in sections where the anoxia event began at this level. Where no anoxia occurred, as in Iran, the ostracod and small foraminifer eurytherm benthos was only marginally affected at the base of the Boundary Clay, and these forms persisted throughout the interval from the base of the *C. meishanensis–H. praeparvus* Zone to the very base of the *H. parvus* Zone (event 6). Therefore, event 6 cannot be found in sections that experienced anoxia starting at the base of the Boundary Clay, because there the extinction of the eurytherm benthos was not caused by the Permian–Triassic biotic crisis, but by the anoxia, which happened also at any other stratigraphic level, where anoxia began. This made the PTB extinction of eurytherm benthos that occurred elsewhere effectively invisible at those localities.

4. Discussions and conclusions: implications for the causes of the Permian–Triassic biotic crisis

The extinction pattern at the major extinction event at base of the Boundary Clay is identical to the extinction pattern at the base of the cool water horizon in the lower *C. zhangi* Zone. As the latter short and rapid cooling event is clearly connected to an especially strong eruptive phase of the Siberian Trap (see above), a connection between the

major extinction event at the base of the Boundary Clay and a volcanic winter is probable (Kozur, 1998a,b). As cosmic microsphaerules are very common in the lower Boundary Clay and contemporaneous beds in the Germanic Basin, an additional stress effect from a bolide impact in the sea cannot be excluded. This would have produced huge tsunamies that in turn may have caused the high-energy event at the base of the Boundary Clay, which can be traced throughout the Tethys region. It is also possible, however, that a huge explosion of a volcanic island and/or related earthquakes could have generated giant tsunamies. In either case, if there were a combined volcanic and cosmic winter, the effect would be the same: a short interval of cooling in low latitudes caused by a strong reduction of sunlight onto the Earth's surface.

A very high level of global anoxia (superanoxia sensu Isozaki, 1994) cannot be the primary cause of this extinction event as assumed by Wignall and Hallam (1992, 1993), Hallam (1994), and Hallam and Wignall (1997). This was not a global event, because it was not present in the greater part of the Neotethys (e.g., Iran and Transcaucasia). Where this event was not present, and the PTB event lies in beds with oxygen-rich bottom waters such as in Iran, the main extinction event still is at exactly the same level whether it is in sections with anoxia or without it.

The most significant characteristics of the PTB biotic crisis were the strongly delayed recovery of 1) a diverse warm water benthos, 2) a diverse low latitude siliceous plankton (radiolarians), and 3) a diverse and dense land vegetation. These recoveries began in the Spathian but were not finished until the Middle Triassic. The interval of extinction and delayed recovery coincides with major perturbations of the carbon cycle (Payne et al., 2004; Korte and Kozur, 2005b; Korte et al., 2005). These include a number of pronounced negative and positive excursions of $\delta^{13}C_{org}$, including a especially pronounced minimum around the PTB, a second minimum in the lower *I. isarcica* Zone, a strong maximum in the basal Smithian, two pronounced minima in the upper Smithian and lower-middle Spathian on either side of a recovery around the Smithian–Spathian boundary, and a maximum around the base of the Anisian. The real biotic recovery, to a diversity level comparable to or higher than what existed before the PTB biotic crisis, did not occur until after the perturbations had ended for a prolonged interval of time (Payne et al., 2004).

The gradual drop of the carbon isotope curve from the *C. nodosa* to the *H. parvus* Zones, over a time interval of about 450,000 years, indicates that neither the carbon isotope excursions nor the PTB biotic crisis were sudden events. Rather, they reflect the culmination of very stressful ecological conditions that also produced the extraordinarily short duration of the conodont zones from the *C. nodosa* to the *H. parvus* Zones. This sequence of events precludes a single and sudden catastrophic event, such as a cosmic impact or an abrupt overturn of a stratified ocean, as the sole cause of the PTB event. Such events by themselves can neither account for the recurring perturbations of the carbon cycle nor the prolonged biotic crisis around the PTB. It is quite possible, however, that interaction between a catastrophic event (such as the huge intermediate-felsic eruptions in South China at the base of the *C. meishanensis–H. praeparvus* Zone) and a prolonged ecological crisis (most probably caused by the huge Siberian Trap volcanic event) may have delivered the *coup de grâce* to an ecosystem already in crisis.

Acknowledgements

The investigations around the Permian–Triassic boundary of Iran were sponsored by the Deutsche Forschungsgemeinschaft (DFG) in Bonn, and by the Geological Survey of Iran at Tehran and Tabris. The field work was guided and/or supported by Dr. S. Bagheri, Lausanne, Prof. Dr. B. Hamdi, Tehran, Prof. Dr. H. Partoazar, Tehran, Dr. R. Aminiazar, Tabris, Dr. T. Mohtat, Tehran, Dr. B. Momeni, Tehran, Dr. B. Sedghi, Tehran, Dr. D. Weyer, Berlin and Prof. M. Yazdi, Esfahan. The work was enthusiastically supported by Prof. Dr. G. Bachmann (Halle), Prof. Dr. H. Mostler (Innsbruck), and Prof. Dr. G. Stampfli (Lausanne), and by Prof. Wang Cheng-yuan (Nanjing). Some of the samples were dissolved and picked by Dr. P. Mohtat (Innsbruck) (Shahreza section) and Dr. C. Korte (Bochum) (Abadeh sections), who investigated also the stable isotopes and made some SEM photographs in the Ruhr University, Bochum. The samples from all other sections and the samples from the second sampling in the Abadeh and Shahreza sections were dissolved and picked out by the author in the Institut für Geologische Wissenschaften in Halle, and in the Geological Institute of the Lausanne University (UNIL). The DFG provided a microscope for study of the conodonts. Most of the SEM photographs were taken by the author at the Institute of Geology and Palaeontology, Innsbruck University with a grant from the Austrian FWF (project no. P 14490-GEO). Dr. P. Ozsvárt in ELTE, Budapest, took some additional SEM photographs. Dr. R. E. Weems, Reston, greatly improved the English. Prof. Yin Hongfu, Wuhan made important suggestions which have greatly improved the final manuscript. I thank very much all mentioned colleagues and institutions for their important help.

References

Baghbani, D., 1993. The Permian sequence in the Abadeh region, central Iran. Occ. Publ. ESRI, N.S., vol. 9 B, pp. 7–22.

Bachmann, G.H., Kozur, H.W., 2004. The Germanic Triassic: correlations with the international scale, numerical ages and Milankovitch cyclicity. Hallesches Jahrb. Geowiss., B 26, 17–62.

Chengyuan Wang, Zhihao Wang, 1981. Conodonts. In: Zhao, Jin-ke, Sheng, Jin-zhang, Yao, Zhao-qi, Liang, Xi-luo, Chen, Chu-zhen, Rui, Lin, Liao, Zhuo-ting (Eds.), The Changhsingian Stage and Permian–Triassic boundary of South China. Bull. Nanjing Inst. Geol. Palaeont. Acad. Sinica, vol. 2, pp. 79–81.

Gallet, Y., Krystyn, L., Besse, J., Saidi, A., 2000. New constraints on the Upper Permian and Lower Triassic geomagnetic polarity time scale from the Abadeh section (central Iran). J. Geophys. Res. 105 (B2), 2805–2815.

Hallam, A., 1994. The earliest Triassic as an anoxic event, and its relationship to the end-Paleozoic mass extinction. Can. Soc. Petrol. Geol., Mem. 17, 797–804.

Hallam, A., Wignall, P.B., 1997. Mass extinctions and their aftermath. Oxford University Press, Oxford–New York–Tokyo. 320 pp.

Henderson, C., Baud, A., 1997. Correlation of the Permian–Triassic boundary in Arctic Canada and comparison with Meishan, China. In: Naiwen, W., Remane, J. (Eds.), Proceedings of the 30th International Geological Congress, vol. 11, pp. 143–152.

Iranian–Japanese Research Group (I–JRG), Taraz, H., et al., 1981. The Permian and the Lower Triassic systems in Abadeh region, central Iran. Mem. Fac. Sci., Kyoto Univ., Ser. Geol. Mineral. 47 (2), 61-13.

Isozaki, Y., 1994. Superanoxia across the Permo–Triassic boundary: record in accreted deep-sea pelagic chert in Japan. Can. Soc. Petrol. Geol., Mem. 17, 805–812.

Jin, Y.G., Wang, Y., Wang, W., Shang, Q.H., Cao, C.Q., Erwin, D.H., 2000. Pattern of marine mass extinction near the Permian–Triassic boundary in South China. Science 289, 432–436.

Korte, C., Kozur, H.W., 2005a. Carbon isotope stratigraphy across the Permian/Triassic boundary at Jolfa (NW-Iran), Peitlerkofel (Sass de Pütia, Sass de Putia), Pufels (Bula, Bulla), Tesero (all three Southern Alps, Italy) and Gerennavár (Bükk Mts., Hungary). J. Alpine Geol. 47, 119–135.

Korte, C., Kozur, H.W., 2005b. Carbon isotope trends in continental lake deposits of uppermost Permian to Lower Olenekian: Germanic Lower Buntsandstein (Calvörde and Bernburg Formations). Hallesches Jahrb. Geowiss., Reihe B, Beiheft 19, 87–94.

Korte, C., Kozur, H.W., Joachimski, M.M., Strauss, H., Veizer, J., Schwark, L., 2004a. Carbon, sulfur, oxygen and strontium isotope records, organic geochemistry and biostratigraphy across the Permian/Triassic boundary in Abadeh, Iran. Int. J. Earth Sci. (Geol. Rdsch.) 93, 565–581.

Korte, C., Kozur, H.W., Mohtat-Aghai, P., 2004b. Dzhulfian to lowermost Triassic $\delta^{13}C$ record at the Permian/Triassic boundary section at Shahreza, Central Iran. Hallesches Jahrb. Geowiss., Reihe B, Beiheft 18, 73–78.

Korte, C., Kozur, H.W., Partoazar, H., 2004c. Negative carbon isotope excursion at the Permian/Triassic boundary section at Zal, NW-Iran. Hallesches Jahrb. Geowiss., Reihe B, Beiheft 18, 69–71.

Korte, C., Jasper, T., Kozur, H.W., Veizer, J., 2005. $\delta^{18}O$ and $\delta^{13}C$ of Permian brachiopods: a record of seawater evolution and continental glaciation. Palaeogeogr. Palaeoclimatol. Palaeoecol. 224, 333–351.

Kozur, H., 1975. Beiträge zur Conodontenfauna des Perm. Geol.-Paläontol. Mitt. Innsbruck 5 (4), 1–44.

Kozur, H., 1978. Beiträge zur Stratigraphie des Perms. Teil II: Die Conodontenchronologie des Perms. Freib. Forsch.-H. C 334, 85–161.

Kozur, H., 1985a. Biostratigraphic evaluation of the Upper Paleozoic conodonts, ostracods and holothurian sclerites of the Bükk Mts. Part II: Upper Paleozoic ostracods. Acta Geol. Hung. 28 (3–4), 225–256.

Kozur, H., 1985b. Neue Ostracoden-Arten aus dem oberen Mittelkarbon (höheres Moskovian), Mittel-und Oberperm des Bükk-Gebirges (N-Ungarn). Geol. Paläontol. Mitt. Innsbruck, Sb. 2, 1–145.

Kozur, H., 1988. The Permian of Hungary. Z. Geol. Wiss. 16 (11/12), 1107–1115.

Kozur, H., 1995. Permian conodont zonation and its importance for the Permian stratigraphic standard scale. Geol. Paläont. Mitt. Innsbruck 20, Festschrift zum 60. Geburtstag von Helfried Mostler, pp. 165–205.

Kozur, H.W., 1998a. Some aspects of the Permian–Triassic boundary (PTB) and of the possible causes for the biotic crisis around this boundary. Palaeogeogr. Palaeoclimatol. Palaeoecol. 143, 227–272.

Kozur, H.W., 1998b. Problems for evaluation of the scenario of the Permian–Triassic boundary biotic crisis and its causes. Geol. Croat. 51 (2), 135–162.

Kozur, H.W., 2003. Integrated ammonoid, conodont and radiolarian zonation of the Triassic. Hallesches Jahrb. Geowiss., B 25, 49–79.

Kozur, H.W., 2004a. Pelagic uppermost Permian and the Permian–Triassic boundary conodonts of Iran, Part I: Taxonomy. Hallesches Jahrb. Geowiss., Beiheft 18, Festschrift zum 60. Geburtstag von Herrn Prof. Dr. Gerhard H. Bachmann, Teil I, 39–68.

Kozur, H.W., 2004b. The age of the palaeomagnetic reversal around the Permian–Triassic boundary. Permophiles 43, 25–31.

Kozur, H.W., 2005. Pelagic uppermost Permian and the Permian–Triassic boundary conodonts of Iran. Part II: Investigated sections and evaluation of the conodont faunas. Hallesches Jahrb. Geowiss., Beiheft 19, Festschrift zum 60. Geburtstag von Herrn Prof. Dr. Gerhard H. Bachmann, Teil II, 49–86.

Kozur, H.W., Bachmann, G.H, 2005. Correlation of the Germanic Triassic with the international scale. Albertiana 32, 21–35.

Kozur, H., Mostler, H., Rahimi-Yazd, A., 1975. Beiträge zur Mikropaläontologie permotriadischer Schichtfolgen. Teil II: Neue Conodonten aus dem Oberperm und der basalen Trias von Nord-und Zentraliran. Geol.-Paläontol. Mitt. Innsbruck 5 (3), 1–23.

Lai Xulong, Cui Wie, Wie Xiong, Ruixia Peng, Zhenzuo Liu, 1999. Primary study on late Permian conodont fauna from Xifanli section, Daye County, southeast Hubei Province, China. In: Yin Hongfu, Tong Jinnan (Eds.), Proceedings of the International Conference on Pangea and the Paleozoic–Mesozoic transition. China University of Geosciencs Press, Wuhan, pp. 15–21.

Lozovsky, V.R., Krasilov, V.A., Afonin, S.A., Pomarenko, A.G., Shcherbakov, D.E., Aristov, D.S., Jaroshenko, O.P., Kuchtinov, D.A., Burov, B.V., Buslovikh, A.L., Morkovin, I.V., 2001. O vydelenii novoj pachki v sostave vochminskoj svity nizhnego triasa Moskovskoj Sineklizy. Bjulleten regionalnoj mezhvedomstvennoj stratigraficheskoj komissii po centru i jugu Russkoj platformy, vol. 3, pp. 151–163.

Mei Shilong, Henderson, C.M., 2001. Evolution of Permian conodont provincialism and its significance in global correlation and paleoclimate implication. Palaeogeogr. Palaeoclimatol. Palaeoecol. 170, 237–260.

Mei Shilong, Zhang Kexin, Wardlaw, B.R., 1998. A refined succession of Changhsingian and Griesbachian neogondolellid conodonts from the Meishan section, candidate of the global stratotype section and point of the Permian–Triassic boundary. Palaeogeogr. Palaeoclimatol. Palaeoeol. 143, 213–226.

Payne, J.L., Lehrmann, D.J.,Wie Jiayong, Orchard, M.J., Schrag, D.P., Knoll, A.H., 2004. Large pertubations of the carbon cycle during recovery from the end-Permian extinction. Science 305, 506–509.

Rostovtsev, K.O., Azaryan, N.R., 1971. The Permian–Triassic boundary in Transcaucasia. Bull. Can. Petrol. Geol. 19, 349–350.

Rostovtsev, K.O., Azaryan, N.R., 1973. The Permian–Triassic boundary in Transcaucasia. In: Logan, A., Hills, L.V. (Eds.), The Permian and Triassic systems and their mutual. Canadian Soc. petrol Geologists, Mem., vol. 2, pp. 89–98.

Ruzhentsev, V.E., Sarycheva, T.G., (Eds.), 1965. Razvitie i smena morskich organismov na rubezhe paleozoja i mezozoja. Trudy Palent. Inst. AN SSSR, vol. 108. 431 pp.

Schenck, H.G., Hollis, D., Hedberg, C.W., Tomlinson, J., Eaton, E., White, R.T., et al., 1941. Stratigraphic nomenclature. Bull. Am. Assoc. Petrol. Geol. 25 (12), 2195–2202.

Scholger, R., Mauritsch, H.J., Brandner, R., 2000. Permian–Triassic boundary magnetostratigraphy from the Southern Alps (Italy). Earth Planet. Sci. Lett. 176, 495–508.

Stampfli, G.M., Borel, G.D., 2004. The TRANSMED transects in space and time. Constraints on the paleotectonic evolution of the Mediterranean Domain. In: Cavazza, W., Roure, F., Spakman, W., Stampfli, G.M., Ziegler, P. (Eds.), The TRANSMED Atlas: The Mediterranean region from crust to mantle, 53.80. Springer, Verlag.

Stepanov, D.L., Golshani, F., Stöcklin, J., 1969. Upper Permian and Permian–Triassic boundary in North Iran. Geol Surv. Iran, Report No. 12. 72 pp.

Sweet, W.C., Mei, Shilong, 1999a. The Permian Lopingian and basal Triassic sequences in northwest Iran. Permophiles 33, 14–20.

Sweet, W.C., Mei, Shilong, 1999b. Conodont succession of Permian Lopingian and basal Triassic in northwest Iran. In: Hongfu, Yin, Jinnan, Tong (Eds.), Proceedings on the International Conference on Pangea and the Paleozoic–Meoszoic transition. China University of Geosciences Press, Wuhan, pp. 43–47.

Szurlies, M., 2004. Magnetostratigraphy: the key to a global correlation of the classic Germanic Trias— case study Volpriehausen Formation (Middle Buntsandstein) Central Germany. Earth Planet. Sci. Lett. 227, 395–410.

Szurlies, M., Kozur, H.W., 2004. Preliminary palaeomagnetic results from the Permian–Triassic boundary interval, Central and NW Iran. Albertiana 31, 41–46.

Takemura, A., Sakai, M., Yamakita, S., Kamata, Y., Aita, Y., Sakai, T., Suzuki, N., Hori, S.R., Sakakibara, M., Kodama, K., Takemura, S., Sakamoto, S., Ogane, K., Koyano, T., Satake, A., Nakamura, Y., Campbell, H.J., Spörli, K.B., 2003. Early Triassic radiolarians from arrow rocks in the Waipapa Terrane, Northern Island, New Zealand. Interrad 2003, Uni Lausanne, Abstracts and Programme, 64.

Taraz, H., 1969. Permo–Triassic section in Central Iran. Am. Assoc. Petrol. Geol. Bull. 53 (12), 688–693.

Taraz, H., 1971. Uppermost Permian and Permo–Triassic transition beds in central Iran. Am. Assoc. Petrol. Geol. Bull. 55 (8), 1280–1294.

Taraz, H., 1973. Correlation of the uppermost Permian in Iran, Central Asia, and South China. Am. Assoc. Petrol. Geol. Bull. 57 (6), 1117–1133.

Taraz, H., 1974. Geology of the Surmaq-Deh Bid area, Abadeh region, Central Iran. Geol. Surv. Iran., Rep. 37. 148 pp.

Teichert, C., Kummel, B., Sweet, W., 1973. Permian–Triassic strata, Kuh-E-Ali Bashi, northwestern Iran. Bull. Mus. Comp. Zool. 145 (8), 359–472 Cambridge.

Veevers, J.J., Conaghan, P.J., Shaw, S.E., 1994. Turning point in Pangean environmental history at the Permian–Triassic boundary. Geol. Soc. Am., Spec. Pap. 288, 187–196.

Wardlaw, B.R., 2004. New ranges– *Clarkina* species– Changxing Limestone, Meishan. —e-mail report to the members of the ISPS, 1 p.

Wardlaw, B.R., Davydov, V.I., 2005. Progress report of the Permian–Triassic time slice project. Permophiles 45, 36–39.

Wignall, P.B., Hallam, A., 1992. Anoxia as a cause of the Permian/Triassic mass extinction: facies evidence from northern Italy and the western United States. Palaeogeogr. Palaeoclimatol. Palaeoecol. 93, 21–46.

Wignall, P.B., Hallam, A., 1993. Griesbachian (earliest Triassic) palaeoenvironmental changes in the Salt Range, Pakistan and southeast China and their bearing on the Permo–Triassic mass extinction. Palaeogeogr. Palaeoclimatol. Palaeoecol. 102, 215–237.

Yamakita, S., Takemura, A., Aita, Y., Sakai, T., Kamata, Y., Suzuki, N., Hori, S.R., Sakakibara, M., Fujiki, T., Ogane, K., Takemura, S., Sakamoto, S., Kodama, K., Nakamura, Y., Campbell, H.J., Spörli, K.B., 2003. Conodont-based age determination for a radiolarian-bearing Lower Triassic chert sequence in Arrow Rocks, New Zealand. Interrad 2003, Uni Lausanne, Abstracts and Programme, 108.

Yazdi, M., Shirani, M., 2002. First research on marine and nonmarine sedimentary sequences and micropaleontologic significance across Permian/Triassic boundary in Iran (Isfahan and Abadeh). J. China Univ. Geosci. 13 (2), 172–176.

Yin, H.F., Huang, S.J., Zhang, K.X., Hansen, H.J., Yang, F.Q., Ding, M.H., Bie, X.M., 1992. The effects of volcanism on the Permo–Triassic mass extinction in South China. In: Sweet, W.C., Yang, Z.Y., Dickins, J.M., Yin, H.F. (Eds.), Permo–Triassic events in the eastern Tethys. Cambridge Univ. Press, Cambridge, pp. 146–157.

Yin, H., Sweet, W.C., Glenister, B.F., Kotlyar, G., Kozur, H., Newell, N.D., Sheng, J., Yang, Z., Zakharov, Y.D., 1996a. Recommendation of the Meishan section as Global Stratotype Section and Point for basal boundary of Triassic System. Newsl. Stratigr. 34 (2), 81–108.

Yin, Hongfu, Wu, Shunbao, Meihua, Ding, Zhang, Kexing, Tong, Jinnan, Yang, Fengqing, Lai, Xulong, 1996b. The Meishan section, candidate of the Global Stratotype Section and Point of Permian–Triassic boundary. In: Yin, Hongfu (Ed.), NSFC Project No. 49472087. The Palaeozoic–Mesozoic boundary candidates of Global Stratotype Section and Point of the Permian–Triassic Boundary. China University of Geosciences Press, pp. 31–48.

Yin, Hongfu, Zhang, Kexin, 1996. Eventostratigraphy of the Permian–Triassic boundary at Meishan section, South China. In: Hongfu, Yin (Ed.), The Palaeozoic–Mesozoic boundary. Candidates of global stratotype section and point of the Permian–Triassic boundary. China University of Geosciences Press, Wuhan, pp. 84–96.

Yin, Hongfu, Zhang, Kexin, Tong, Jinnan, Yang, Zunyi, Wu, Shunbao, 2001. The Global Stratotype Section and Point (GSSP) of the Permian–Triassic boundary. Episodes 24 (2), 102–114.

Zakharov, Y.D., Sokarev, A.N., 1991. Biostratigrafija i paleomagnetism permi i triasa Evrazii. AN SSSR, Dalnevostochnoe otdelenie. Dalnevostochnyj Geologicheskij Institut. Moskva, Nauka. 135 pp.